Molecular, isotopic and radiocarbon evidence for broomcorn millet cropping in Northeast France since the Bronze Age

Blandine Courel, Philippe Schaeffer, Pierre Adam, Estelle Motsch, Quentin Ebert, Emile Moser, Clément Féliu, Stefano M. Bernasconi, Irka Hajdas, Ertlen Damien, et al.

Molecular, isotopic and radiocarbon evidence for broomcorn millet cropping in Northeast France since the Bronze Age

Blandine Courel[a], Philippe Schaeffer[a*], Pierre Adam[a], Estelle Motsch[a], Quentin Ebert[a], Emile Moser[a], Clément Féliu[b,c], Stefano M. Bernasconi[d], Irka Hajdas[e], Damien Ertlen[f], Dominique Schwartz[f]

[a] *Université de Strasbourg, CNRS, CHIMIE, UMR 7177, F-67000 Strasbourg, France*

[b] *Inrap Grand-Est Sud, 67100 Strasbourg, France*

[c] *Université de Strasbourg, Université de Haute Alsace, CNRS, ArchIMèdE UMR 7044, F-67000 Strasbourg, France*

[d] *Geologisches Institut, ETH Zürich, Zürich, Switzerland*

[e] *Laboratory of Ion Beam Physics, ETH Zürich, Zürich, Switzerland*

[f] *Université de Strasbourg, CNRS, Laboratoire Image, Ville, Environnement UMR 7362, F-67000 Strasbourg, France*

[*]Corresponding author. Tel: +33 (0)3 68 85 28 05.

E-mail address: p.schaef@unistra.fr (Philippe Schaeffer).

ABSTRACT

Molecular and isotopic investigation of lipids from soils filling several structures from an archaeological site located at Obernai (Alsace, NE France) has revealed the presence of miliacin, a triterpenoid marker from *Panicum miliaceum* (broomcorn millet), indicating that this cereal was cultivated at the site. The concentration profiles of miliacin within silos and its detection in other archaeological structures (e.g. Gaulish pit) suggest that miliacin did not originate from cereals stored in the silos but rather came from remains of millet from cultivated soils which filled the silos after they were abandoned. Furthermore, the ^{14}C age of miliacin isolated from a silo of the Second Iron Age was shown to be considerably older (Bronze Age) than the structure itself, revealing that the soil filling the silo therefore archived the molecular signature from past millet cropping, predating the digging of the silo. Thus, radiocarbon dating of the isolated miliacin allowed the timing of millet cropping to be determined, showing that it was established during the Bronze Age and the Roman Gaul period at Obernai. This is the first evidence of millet cultivation in Alsace dating back to the Bronze Age, bringing new perspectives on agricultural and past dietary practices in Eastern France. The combination of molecular studies and radiocarbon dating of individual lipids highlights the potential of hollow structures like silos and pits to act as "pedological traps", recording information on past vegetation cover or agricultural practices from the surface horizons of surrounding soils that filled these structures after abandonment.

Keywords (3-7 words): *Panicum miliaceum*; miliacin; compound-specific radiocarbon analysis; archaeometry; soil lipids; pedological traps.

1. Introduction

When chemical analytical techniques were initially introduced to archaeological research during the middle of the 20th century in a discipline referred to as archaeometry, the analysis mainly involved characterization of organic residues and materials related to artifacts such as pottery and jars (Condamin et al., 1976; Evershed et al., 1991; Charters et al., 1995; Charrié-Duhaut et al., 2007), hafting material on flints (Boëda et al., 1996) or mummies (Connan, 1999; Buckley and Evershed, 2001). It is only more recently that lipid biomarkers in organic matter (OM) preserved in soils and sediments have been considered as archaeological archives (e.g. Bull et al., 2001; Egli et al., 2013; Motuzaite-Matuzeviciute et al., 2016). These lipids, which possess relative stability and resistance towards biodegradation (Eglinton and Logan, 1991; Lorenz et al., 2007), have been shown to have a potential as chemotaxonomic markers, allowing a link to be established between the preserved molecules ("chemical fossils") and their source organisms. Thus, lipid biomarkers, preserved within palaeosoils and sediments, may represent valuable tools for reconstructing palaeoenvironments or studying the evolution of landscapes through time (Trendel et al., 2010; Lavrieux et al., 2012; Ertlen et al., 2015), or investigating ancient dietary and agricultural practices (Bull et al., 1999; Jacob et al., 2008a; Sistiaga et al., 2014; Motuzaite-Matuzeviciute et al., 2016) or other human activities such as hemp retting (Lavrieux et al., 2013).

In studies dealing with soils, the lipid compartment of soil OM (SOM) is a result of the combination of old and refractory compounds mixed with more recent lipid inputs originating from the vegetation cover of the topsoil and introduced into deeper horizons by processes such as bioturbation, leaching or root penetration (Kögel-Knabner, 2002; Schmidt et al., 2011). Furthermore, the role of microorganisms living within the soil ecosystem has to be considered since they consume and produce part of the soil lipid components (Kögel-Knabner, 2002). The lipid content of SOM also depends strongly on the degree of preservation, which is related to

66 different factors such as climate, biological activity, pH, level of oxygenation, depth,
67 mineralogy, or biochemical nature of the soil (Schmidt et al., 2011). As a result of the intense
68 reshuffling of SOM and of the differential inherent persistence of the various lipid constituents
69 of soils, interpretation of the lipid signatures from soils in terms of archaeological significance
70 and their relationship with a chronological sequence is difficult to establish (Schwartz, 2012).
71 In this respect, radiocarbon dating of SOM, lipid fractions and, in more rare instances,
72 individual compounds from soils represents a powerful tool, potentially allowing, in the case
73 of lipids, specific molecular signatures to be related to a chronological/historical context (e.g.,
74 Rethemeyer et al., 2005; Mendez-Milan et al., 2014). The tremendous advances in ^{14}C
75 instrumentation during the last decade enable samples containing only minute amounts of
76 carbon to be dated (e.g., Ingalls and Pearson, 2005; Birkholz et al., 2013; Gierga et al., 2016).
77 In particular, the accelerator mass spectrometry (AMS) facility MICADAS (MIni CArbon
78 DAting System), designed and developed at the ETH of Zurich, is equipped with a gas handling
79 system and a gas ion source, allowing direct radiocarbon measurement of CO_2 obtained via
80 oxidation of very small samples, thereby giving access to radiocarbon dating of single
81 compounds at the microgram scale (Ruff et al., 2007, 2010).

82 In the present study, we have investigated the content of lipid extracts (LEs) from soil material
83 filling archaeological structures (silos, pit and latrines)near the city of Obernai (Alsace, NE
84 France) using gas chromatography-MS (GC-MS) and GC-combustion- isotope ratio MS (GC-
85 *c*-IRMS),The investigation, which was originally aimed at determining the nature of the
86 cereals/plants that could have been stored in the silos and potentially cultivated at the site, has
87 revealed the presence of miliacin, a triterpenoid marker from *Panicum miliaceum* (broomcorn
88 millet). Its occurrence and significance in terms of preservation and timing of millet cultivation
89 is discussed, notably in the light of the stable carbon isotopic composition of lipids and
90 radiocarbon dating of isolated miliacin.

2. Material and methods

2.1. Samples and archaeological context

The archaeological site of Obernai (Alsace, NE France), spread over more than 7.5 hectares, was excavated in 2013 by the Institut National de Recherche Archéologique Préventive (INRAP) and has yielded numerous pieces of evidence for successive periods of human occupation dating back from the Neolithic period up to the beginning of the Middle Ages (Féliu et al., unpublished results). Among the structures unearthed, some corresponded to protohistoric silos deeply buried in the loess substrate (ca. 1-2.2 m high by ca. 1.5-2 m wide; Fig. 1 and Fig. S1 in Supplementary data). The silos, which were used for cereal storage, indicate that local agricultural activity occurred at the site. Some of the silos, dated from the Late Bronze Age (950-800 BC) and Second Iron Age (La Tène B, 400-260 BC), based on the typology of the ceramics in the soils filling the silos, were selected for biomarker analysis (Table 1). In addition, soil samples from one Neolithic silo (4600-4300 BC), one silo dated from La Tène D (150-30 BC), as well as from a Gaulish pit encircling a farm and Roman Gaul latrines (end of the 2nd centuary AD – beginning of the 3rd centuary AD) were collected (Table 1). In the case of the silos, soil samples were collected at different depth levels within the apparent archaeological layers (ALs; Fig. 1 and Fig. S1 in Supplementary data). For comparison, the loess soils within which the silos were dug - named "loess substrate" (LS)- were sampled.

2.2. Reference material from P. miliaceum

Lipids from reference plant samples from *P. miliaceum* (broomcorn millet) provided by J. Jacob (Institut des Sciences de la Terre d'Orléans) were investigated. They consisted of seeds, stems, ears, leaves and roots obtained from millet cultivated in the frame of a detailed study of millet (Bossard et al., 2013).

114 *2.3. Cautions taken during the sample treatment*

115 In order to avoid contaminations (e.g., phthalates), all commercial solvents were redistilled and
116 stored in glass bottles carefully cleaned and closed with an aluminium foil. Prior to use, all
117 glasswares were washed using water, acetone and finally with redistilled dichloromethane. All
118 equipements/supplies (pipettes, sand, silica, celilte) were washed with dichloromethane in a
119 Soxhlet. Once cleaned, the silica gel was activated at 120 °C. Each samples was kept in a freezer
120 at -20 °C.

121 *2.4. Lipid extraction and fractionation (general procedure)*

122 Lipids from archaeological soils (ca. 500 g) and from plant reference material were extracted
123 via sonication using CH_2Cl_2/CH_3OH (1:1, v/v) followed by filtration of the supernatant through
124 celite and solvent removal under reduced pressure. In the case of archaeological soils, the yield
125 of lipid extract (LE) was low (≤ 0.04% of soil). Derivatization and fractionation of an aliquot
126 of the extract was carried out after Schnell et al. (2014). Briefly, following acetylation of the
127 alcohol functionalities using an excess of Ac_2O and 20 µl of *N*-methylimidazole (catalyst) and
128 methylation of the carboxylic acids using CH_2N_2 in Et_2O, the derivatized crude extract was
129 fractionated on a silica gel column into an apolar fraction eluted with CH_2Cl_2/EtOAc (8:2, v/v)
130 and a more polar fraction eluted with CH_2Cl_2/CH_3OH (1:1, v/v), the latter not being investigated
131 further. After solvent extraction and prior to derivatization and fractionation, the propyl ester
132 of stearic acid was added as internal standard (IS) for quantitative analysis of miliacin.

133 *2.5. Lipid fractionation and derivatization for stable carbon isotope measurements*

134 *2.5.1. Fractionation of the LE*

135 An aliquot of the underivatized lipid extract adsorbed onto silica gel was fractionated using
136 activated silica gel column chromatography, eluting successively with cyclohexane/CH_2Cl_2

(9:1, v/v; 1 dead volume, V_0) to yield the hydrocarbon fraction, followed by CH_2Cl_2 (2 x V_0) to provide mainly miliacin, then CH_2Cl_2/EtOAc (9:1, v/v; 2 x V_0) for the *n*-alcohols and sterols. Finally, the most polar components, comprising carboxylic acids, were recovered with CH_2Cl_2/CH_3OH (1:1, v/v; 2 x V_0).

2.5.2. Derivatization

The alcohol fraction, dissolved in CH_2Cl_2, was derivatized using pyridine (40 µl) and *bis*-(*N,O*-trimethylsilyl)trifluoroacetamide (BSTFA; 70 °C, 2 h), the $\delta^{13}C$ composition of the trimethylsilyl (TMS) group having been determined previously. The solvent and excess reagent were removed under a stream of N_2.

The polar fraction was reacted with BF_3/CH_3OH (the $\delta^{13}C$ value of CH_3OH being known) at 60 °C for 2 h. The crude mixture was then transferred to a separatory funnel and the organic layer recovered after addition of distilled water and CH_2Cl_2. After removal of CH_2Cl_2 under reduced pressure, the derivatized extract was filtered through a small silica gel column/pipette using CH_2Cl_2, yielding the fatty acid (FA) methyl ester fraction.

The known isotopic composition of the added TMS group ($\delta^{13}C$, -20.8‰) and CH_3OH group ($\delta^{13}C$, -48.5‰) allowed the $\delta^{13}C$ value of the derivatized lipids to be corrected using the following equation (Rieley, 1994):

$$\delta_c = (n_{cd}\delta_{cd} - n_d\delta_d)/\, n_c$$

with *n* the number of carbon and δ the carbon isotopic ratio for derivatized compounds (*cd*), the derivative group added (*d*) and the compound prior to derivatization (*c*).

2.6. Decarbonation of soil samples

For radiocarbon dating and $\delta^{13}C$ determination of SOM, an aliquot of the soil sample was decarbonated using 6 N HCl at room temperature (15 min). After centrifugation, the supernatant was removed by pipetting and the residue rinsed with distilled water. The procedure was repeated until neutral and the residue oven-dried at 50 °C.

2.7. Isolation of miliacin

The LE from selected samples (Table 1) was fractionated on a silica gel column, eluting successively with cyclohexane/CH_2Cl_2 (8:2), CH_2Cl_2 and CH_2Cl_2/CH_3OH (1:1), the second-eluted fraction being enriched in miliacin, as shown from GC-MS analysis (Fig. S2 in Supplementary data). This fraction was further purified and manually collected using high performance liquid chromatography (HPLC) with a Waters model 590 HPLC pump (mobile phase: CH_2Cl_2/CH_3OH, 2:8, v/v; flow rate, 1 ml/min), connected to an Agilent ZORBAX SB-C18 column (25 cm x 4.6 mm i.d., 5 µm, Agilent) and associated with a differential refractometer detector R401 (Waters Associates). After a control of the purity of the miliacin sample using GC flame ionization detection (GC-FID) , a final clean up step using silica gel thin layer chromatography (TLC, 0.5 mm SiO_2) was sometimes required (samples 1330.AL2, 6, 10) and carried out using cyclohexane/Me_2CO (98:2) as developer, miliacin having a retention factor between 0.76 and 0.83. The final purity was checked using GC-FID and GC-MS (Fig. S2, Supplementary data).

2.8. GC-MS

GC-MS was carried out with a Thermo Trace gas chromatograph (Thermo Scientific) equipped with Tri Plus autosampler, a programmed temperature vaporizing (PTV) injector and a HP5-MS column (30 m x 0.25 mm i.d. x 0.25 µm film thickness) using He as carrier gas (constant 1.1 ml/min). The temperature program used a gradient from 70 °C to 200 °C at 10 °C/min, then from 200 °C to 300 °C at 3 °C/min (conditions A) or at 4°C/min (conditions B) followed by

182 isothermal at 300 °C for 40 min. The GC equipment was coupled to a Thermo TSQ Quantum
183 mass spectrometer working in the electron ionization (EI) mode at 70 eV and scanning *m/z* 50
184 to 700. The data were investigated using the Xcalibur Software and mass spectra were
185 compared with the NIST library and literature data (for MS data, see Table S1 in Supplementary
186 data).

187 *2.9. GC-FID*

188 GC-FID was carried out with a HEWLETT-PACKARD HP 6890 gas chromatograph equipped
189 with an on-column injector, FID and a HP5-MS column (30 m x 0.32 mm i.d. x 0.25 µm film
190 thickness). The temperature program was: 70 °C – 300 °C (held 40 min) at 10 °C/min), with H_2
191 as carrier gas (constant 2.5 ml/min). The temperature of the detector was 310 °C.

192 *2.10. Elementar analysis-combustion-isotope ratio mass spectrometry (EA-c-IRMS)*

193 Bulk carbon isotope composition ($\delta^{13}C$) of SOM was determined using an Elementar Vario
194 Micro Cube equipped with thermal conductivity detection and coupled to an Isoprime visION
195 stable isotope ratio mass spectrometer. Homogenized decarbonated soil samples were weighted
196 into Sn capsules using a microbalance (2 $x10^{-2}$g; CPA26P Sartorius). The capsules were
197 individually introduced into a combustion furnace (950 °C) with an excess of O_2. CuO was used
198 as the oxidation catalyst and He was the carrier gas. Water was removed with a P_2O_5 trap and
199 CO_2 was separated with a purge and trap desorption column. Ion currents (*m/z* 44, 45, 46) were
200 measured continuously for CO_2 using triple Faraday cups connected to high gain amplifiers.
201 Reference pulse peaks of laboratory CO_2 gas were calibrated against the international standards
202 IAEA C3 ($\delta^{13}C$ = -24.91 (0.49) ‰) and IAEA C4 ($\delta^{13}C$ = -23.96 (0.62) ‰) for CO_2 (IAEA,
203 Vienna, Austria). The isotopic composition of samples was normalized to a calibrated IVA soil
204 standard (1.65% C, $\delta^{13}C$ = -26.66‰) measured under identical conditions every 10 samples.

205 The stable isotope ratio values are given in the delta notation with respect to the standard Vienna
206 Pee Dee Belemnite (VPDB).

207 *2.11. GC-c-IRMS*

208 GC-*c*-IRMS measurements were carried out with a Trace GC Ultra gas chromatograph
209 equipped with an on-column injector, Agilent HP5-MS column (30 m x 0.25 mm i.d. x 0.1 µm
210 film thickness), GC Isolink II conversion unit, comprising a combustion oven (at 1000 °C), a
211 ConFlo IV interface system and a Delta V Plus mass spectrometer (Thermo Scientific). The
212 temperature program was: 80 °C – 310 °C (4°C/min) – isothermal at 310 °C (40 min). Each
213 analysis was repeated 3x and the mean standard deviation was calculated.

214 Before and after each triplicate, the carbon isotopic composition of a certified *n*-alkane mixture
215 (Type A5; Arndt Schimmelmann, Department of Geological Sciences, Biogeochemical
216 Laboratories, Indiana University, USA) was measured and used for calibration. The stability of
217 the measurements was checked using pulses of reference CO_2 prior (5 pulses) and after (3
218 pulses) each run. The data were analyzed using Isodat 3.0 software. For correction of the $\delta^{13}C$
219 values of derivatized lipids, see Section 2.4.

220 *2.12. Radiocarbon dating from AMS*

221 The ^{14}C measurements were performed in the Laboratory of Ion Beam Physics (ETH of Zurich,
222 Switzerland) using the MICADAS AMS equipment (Synal et al., 2007) which possess a gas
223 handling system adapted for very small volumes (µg level; Ruff et al., 2010; Wacker et al.,
224 2010a,b). Samples containing > 100 µg C as well as phthalic acid (blank analyses) were
225 graphitized using the automated AGE system (Wacker et al., 2010a). Small samples (i.e isolated
226 miliacin) were oxidized (combusted) and the resulting CO_2 was transferred to quartz tubes for
227 analysis in the ion source (Ruff et al., 2007, 2010). A standard (oxalic acid II) was prepared and

measured together with the samples. $^{14}C/^{12}C$ and $^{13}C/^{12}C$ isotopic ratios were determined using the MICADAS dating system (Synal et al., 2007; Wacker et al., 2010b). Measured $^{14}C/^{12}C$ values of samples were corrected for the blanks and isotopic fractionation ($\delta^{13}C$, determined with graphite or CO_2), ^{14}C age values were calculated following Stuiver and Polach (1977). Calibrated ages were established using the atmospheric calibration curve IntCal13 reported by Reimer et al. (2013).

3. Results and discussion

3.1. Evidence from miliacin for millet cropping

Overall, at the Obernai site, the lipid signatures from the soils sampled within the silos (e.g. silo 1330; Fig. 2a), in the loess substrate and in the Gaulish pit (structure 1001; Fig. 2b,c) showed the same global lipid assemblage, comprising *n*-alkyl lipids (alkanes, FAs and alcohols), sterols and triterpenoids. *n*-Alcohols in the C_{22}-C_{32} range were predominant and showed an even carbon number predominance, with C_{26} prevailing. Even numbered *n*-acids from higher plants in the C_{20}-C_{32} range were systematically dominated by C_{24}-C_{30}, whereas *n*-alkanes with an odd/even predominance were generally dominated by C_{29} and C_{31}. These straight chain distributions reflect the contribution from terrestrial plants, possibly from grassland plants (e.g. van Bergen et al., 1997; Trendel et al., 2010). Within most silos and in the Gaulish pit and latrines (Fig. 2), C_{29} sterols (**1-3**; numbers refer to structures in Appendix A), as well as a series of pentacyclic triterpenoids comprising glutinone (**4**), taraxerol (**5**), germanicol (**6**), lupeol (**7**), friedelin (**8**), α-amyrin (**9**), bauerenyl acetate (**10**) and betulin (**11**), again point toward a predominant higher plant contribution (e.g. Lavrieux et al., 2011; Schnell et al., 2014). Closer examination of the triterpene assemblage from the soil samples filling some of the archaeological structures (silos, Gaulish pit, latrines; Fig. 2) revealed the presence of an early eluting triterpenoid identified as olean-18-en-3β-ol methyl ether, i.e. miliacin- (**12**), based on

its mass spectrum (Jacob et al., 2008b). This rather rare compound belongs to the series of pentacyclic triterpene methyl ethers (PTMEs) generally restricted to Gramineae (Ohmoto et al., 1970; Jacob et al. 2005). The presence of a methoxy group at C-3 has been shown to give a high resistance of PTMEs towards biodegradation, which additionally display antibacterial and antifungal properties (Jacob et al., 2005). This enhanced resistance allowed miliacin to be detected within palaeosoils investigated in an archaeological context (Motuzaite-Matuzeviciute et al., 2016). As shown by Jacob et al. (2008b) and Bossard et al. (2013), miliacin is closely linked to its specific precursor organism, *Panicum miliaceum* (broomcorn millet or common millet), where it occurs in the different plant compartments (seeds, stems, ears, leaves, roots), but is more concentrated by far in the grains. In contrast, it is completely absent among the triterpenoids from another widespread millet species, *Setaria italica* (foxtail millet; Bossard et al., 2013), allowing a distinction to be made at the molecular level between these two cereal species. Given this specificity, detection of millet within most of the soils filling the silos at the Obernai site is of particular interest. Its presence indeed suggests that common millet was cultivated at the site, with the possibility that this cereal was stored within the silos (see below). Furthermore, other minor triterpenoids also biosynthesized by the broomcorn millet - although in much lower quantity than miliacin - comprising isosawamilletin (**13)** - another PTME - together with germanicol (**6**) and friedelin (**8**) (Bossard et al., 2013), co-occur with miliacin in the archaeological soils (Fig. 2a). Another piece of evidence confirming that millet was present at the site was recently obtained from carpological studies (Durand, unpublished results) which led to the identification of a few carbonized and mineralized grains of *P. miliaceum* within some silos. However, the low number of grains (< 10) generally identified in the different silos - except in the case of silo 1763 in which 172 remnants of carbonized grains were identified in the lower archaeological layer (AL2; Fig. 1) - did not allow a correlation to be established between the occurrence of cereal remains in the silos and the presence of miliacin in the

277 corresponding soil samples. Some silos indeed showed a complete absence of millet grains, but
278 where miliacin was detected. Finally, stable carbon isotopic studies provided additional
279 evidence indicating that miliacin found at Obernai and common millet are closely linked. The
280 $\delta^{13}C$ value of miliacin was determined at ca. -21.5‰ (Table 2), in the same range as the values
281 reported for miliacin isolated from reference millet grains or extracted from soils (-21.5 to -
282 23.5‰; Jacob et al., 2008b). These values, around -20‰, are much less ^{13}C-depleted than those
283 generally determined in the case of lipids from temperate region plants which generally use the
284 C_3 carbon fixation pathway. This pathway leads to lipids having $\delta^{13}C$ values between -30 and -
285 40‰ (e.g. Collister et al., 1994; Chikaraishi et al., 2004; Bi et al., 2005; Chikaraishi and
286 Naraoka, 2006), whereas *P. miliaceum* has a C_4 metabolism (Jacob et al., 2008b). The
287 latterleads to the biosynthesis of biomass (including lipids) less ^{13}C-depleted (e.g., Chikaraishi
288 et al., 2004; Bi et al., 2005; Chikaraishi and Naraoka, 2007; Mendez-Millan et al., 2014). In
289 the case of miliacin detected at the Obernai site, the $\delta^{13}C$ composition is in good agreement
290 with a C_4 plant source, confirming that it most likely originates from *P. miliaceum* (Jacob,
291 2008b).

292 *3.2. Role of archaeological pits as traps for lipid biomarkers*

293 As determined above, based on molecular, isotopic and carpologic grounds, millet seemed to
294 be present and likely cultivated as a cereal at the site of Obernai. Given the presence of miliacin
295 in most of the silos, it can be proposed, at first glance, that millet was stored in the silos, at least
296 in those dating from the Middle Bronze Age (silo 1763) up to the Second Iron Age (silos 1330,
297 1508, 1513 and 1521). If this were the case, miliacin would represent the molecular remains of
298 the grains originally stored in the silos and recovered for consumption. One would then expect
299 to find the highest concentration of miliacin at the bottom of the silos, and eventually trace
300 amounts (if any) in the AL from the middle and upper soil filling. To test this hypothesis,

quantitative analysis of miliacin by way of GC-FID was performed on AL from silo soil samples at different filling depths. Except in the case of silo 1817 (Neolithic), in which no miliacin was found (see discussion below), all LE from the silo soils contained miliacin in high relative amount (Fig. 3), whereas it was absent - or present at trace level - in the loess substrate. This strongly suggests that the presence of miliacin is closely associated with the silos. However, miliacin concentration profiles within the different silos showed high variability. In silos 1513, 1508 and 1763, the highest concentration was at the bottom, whereas the opposite was the case for silos 1521 and 1781 (Fig. 3). There was also an intermediate situation, with the highest concentration in the middle sampling levels (silo 1330). These unexpected concentration profiles suggested that miliacin (and hence, millet cultivation) was closely associated with the surface horizons of surrounding soils that filled the silos rather than indicating that millet was the cereal stored in the silos. This apparent disjunction between the function of an archaeological structure (cereal storage in silos, in the present case) and its lipid content is also illustrated by the presence of miliacin in the LE from a Gaulish pit sample - an archaeological structure not related to any agricultural practices - from the same archaeological site (Fig. 2c).

In conclusion, with respect to the presence of millet at this archaeological site, we propose that the silos, as well as the Gaulish pit, played the role of "archaeological traps", in the sense that these structures, once abandoned, were filled quickly (intentionally or not) with surrounding soil horizon(s), the latter having been "sealed" within these structures and having kept the record of past agricultural practices. This conclusion would be in line with the concept of “pedological trap” recentlydeveloped (e;g., Ertlen et al., 2013; Lauer et al., 2013).

3.3. Evidence from ^{14}C dating for millet cropping dating back to the protohistoric and antic periods

In order to constrain the timing of millet cultivation/consumption at the Obernai site, ^{14}C dating measurements were undertaken on SOM, LE, isolated miliacin from a series of selected archaeological samples and millet grains from silo 1763 (Féliu, 2017). Among them, two silos were chosen as representative of distinct periods of occupation of the site, based on ceramology dating (Table 1). Silo 1763 represents the oldest structure in which miliacin was detected (see above) and is dated from the Late Bronze Age (950-800 BC, corresponding to ca. 2900-2750 yr BP), whereas silo 1330 was selected to cover the Second Iron Age (400-260 BC, ca. 2350-2210 yr BP). A third, more recent structure (4564) from the site - not discussed in detail here - corresponding to latrines from the Roman Gaul period (end of the 2nd - beginning of the 3rd century AD, ca. 1750-1800 yr BP), was also shown to contain exceptionally high amounts of miliacin (Fig. 2d), which was isolated from AL8 and ^{14}C dated (Table 3).

Given the low amount of OM generally in these loess soil samples (TOC < 0.1%), radiocarbon dating measurements were carried out using the AMS instrument MICADAS. Pure miliacin from silos 1330 and 1763 and Roman-Gaul latrines 4564 was obtained from the LE from AL (Table 3) using a combination of separation steps involving silica gel liquid chromatography, reversed phase HPLC and thin layer chromatography (Section 2.6). Using our isolation protocol, miliacin was recovered in the range of 15 µg to 300 µg, with a purity between 80% and > 90% (determined from GC, Fig. S2 in Supplementary data), the co-occurring compounds comprising mainly olean-13(18)-en-3β-ol methyl ether (isosawamilletin, **13**) another triterpenoid from millet (Bossard et al., 2013). Despite the rather low quantity isolated in most cases, ^{14}C age values could be determined as ^{14}C age BP and calibrated ^{14}C age BC (Table 3 and Table S2 for the complete data set).

In the case of silo 1330 (Second Iron Age), the ^{14}C age of SOM from a soil sample collected within AL6 located at mid-depth of the silo (Fig. 1) was measured at 3042 yr BP, slightly older than the lipid extract from the same soil sample by ca. 200 yr (Fig. 4 and Table 3). The age of

miliacin isolated from this soil sample, as well as that from miliacin from two AL located at the bottom and top of the same silo (AL2 and AL10) showed globally the same age of ca. 3000-3200 yr BP (Fig. 4 and Table 3). Interestingly, the ^{14}C age of miliacin from the second silo (silo 1763, Late Bronze Age) was similar to that of miliacin from silo 1330 (Second Iron Age). These values, all close to that determined for SOM from AL6 (silo 1330) and AL2 (silo 1763), are clearly older than the age of silo structure 1330 as determined from ceramology (ca. 400-260 BC), indicating that miliacin (and hence, millet) was not contemporaneous with the use of the silos for cereal storage. In fact, in all cases, the age of miliacin corresponds to the Bronze Age, between 3994 and 2776 yr BP, whereas silos 1763 and 1330 were probably in use between 950-800 BC (end of the Bronze Age) and 400-260 BC (second Iron Age), respectively.

The age difference between the archaeological structure and miliacin was particularly marked with silo 1330, with a difference > 600 yr. Moreover, the similarity in the age of miliacin from the three archaeological layers sampled within silo 1330 indicates that the structure was filled quickly with the same soil after abandoning, whatever the archaeological layers considered. The situation was different with silo 1763, for which miliacin had almost the same (or slightly older) age (Fig. 4) than the silo dated from the end of the Bronze Age, a period during which the cereal was cultivated and likely stored in silos. A confirmation that millet was consumed at this time period was indeed attested to from the presence, at the bottom of the structure (AL2; Fig. 1), of a few carbonized millet grains, dated at ca. 2800 yr BP (2880-2762 cal yr BP for 2σ; Féliu, 2017).

In conclusion, based on quantitative and ^{14}C dating measurements, it appears that the presence of miliacin cannot be interpreted as evidence of cereal storage in the silo structures, contrary to what was initially envisaged, but rather reflects the existence of millet cultivation predating the digging of the silos, except silos 1817 (Neolithic, predating millet cropping), and 1763 (Late Bronze Age, contemporaneous with millet cropping). Once abandoned, the emptied silos were

374 filled rapidly with the surface horizons of surrounding soils and thus acted as "pedological
375 traps" for the soils that were used for millet cultivation ca. 3 kyr BP ago, sealing and preserving
376 their SOM content, including lipids. A search for biomarkers indicative of the contribution of
377 other types of cereals, such as wheat or barley, such as e.g., alkyl resorcinols (Appendix A;
378 Hengtrakul et al., 1991; Seitz, 1992; Ross et al., 2003, 2004), was unsuccessful. Indeed, there
379 was no evidence for such an occurrence from the lipid extracts, whereas these cereals could be
380 detected in the form of carbonized grains from carpological studies, found within some silos
381 dated from the Late Bronze Age and La Tène (Durand, unpublished results). The absence of
382 alkyl resorcinols could be due to a low preservation potential, as these compounds have been
383 shown to be easily degraded upon processes like fermentation or heating (Winata and Lorenz,
384 1997), possibly explaining why they have never been reported in archaeological studies.

385 The case of the Roman Gaul latrine structure 4564 is sharply different from that of the silos,
386 since an almost identical ^{14}C age was obtained for the LE, SOM and miliacin, this age being
387 also in good agreement with that of the structure itself, as determined independently from
388 ceramology. In this case, miliacin consumption (and/or millet cultivation) could be
389 unambiguously correlated with the Roman Gaul period, and was confirmed from carpological
390 studies showing the presence - although in very low amount - of mineralized millet grains
391 within the latrine structure (Durand, unpublished results).

392 *3.4. C_4 vs. C_3 plant input using the $\delta^{13}C$ record of n-alkyl lipids*

393 Several studies have used the C isotopic changes of SOM or lipids within soils to trace back C_3
394 vs. C_4 vegetation change and to study the turnover of SOM induced by the vegetation change
395 (e.g. Schwartz, 1991; Mariotti and Peterschmitt, 1994; Pessenda et al., 1998; Wiesenberg et al.,
396 2004; Quénéa et al., 2006; Mendez-Millan et al., 2014). In the present study, the stable carbon
397 isotopic composition of some straight chain lipids (*n*-alkanes, FAs and alcohols) from selected

soil samples was measured in order to determine if *n*-alkyl inputs from a C_4 plant (i.e., millet) could be detected on the basis of these compounds. It appeared that the *n*-alkanes in the LE from the soils filling silos 1330, 1781 and 1508 showed $\delta^{13}C$ values between -29.9 and -35.5‰ (Table 2) typical for C_3 plants (Bi et al., 2005; Mendez-Millan et al., 2014). The same held for the FAs - when they could be measured - with $\delta^{13}C$ values ranging between -31.6‰ and -37.0‰ (Table 2). Similar values were obtained in the case of the *n*-alcohols ($\delta^{13}C$ between -31.4‰ and -36.8‰; Table 2). These values highlight an almost pure C_3 isotopic signature. This was confirmed by the $\delta^{13}C$ values of bulk SOM in selected samples (silo 1330 AL 2, 6, 10 and Roman latrines 4564 AL 4, 8 9), which all fell in the rather narrow range of -25.5‰ ± 1, corresponding to a C_3 source (e.g. Balesdent et al., 1987; Schwartz, 1991; Beniston et al., 2014; Chikaraishi et al., 2004). Interestingly, the $\delta^{13}C$ values of SOM from the corresponding surrounding soils gave the same isotopic signature, indicating that the C_4 contribution detected at the molecular level (i.e. the presence of miliacin) could not be observed from bulk carbon analysis.

For the lipids, the case of 1-dotriacontanol (*n*-C_{32}) was slightly different from the other straight chain compounds, with a $\delta^{13}C$ value enriched in ^{13}C by ca. 2-4‰ compared with the lower *n*-alcohol C_{26}-C_{30} homologues (Table 2), suggesting a mixed contribution from both C_3 and C_4 plants. This is the case in all the silo samples containing miliacin and, interestingly, not the case for the loess substrate samples and for the Neolithic silo 1817, the sole silo devoid of evidence for millet occurrence (Table 2). It turns out that our study of common millet highlighted the particular abundance of 1-dotriacontanol in the leaves (Fig. S3 in Supplementary data) in accordance with the literature (up to 80% of summed free *n*-alcohols according to Tulloch, 1982). Consequently it could be envisaged that part of this compound coming from millet was preserved, whereas the C_4 $\delta^{13}C$ signature of the other straight chain lipids, originally less

422 abundant in millet, was progressively replaced with the C_3 $\delta^{13}C$ signature of the succeeding
423 vegetation.

424 In conclusion, most of the soil lipids, as well as the SOM showed a clear C_3 plant signal, most
425 likely reflecting the contribution from Gramineae. In the soils filling the silos, this predominant
426 contribution was accompanied by a small signal from a C_4 plant source, mainly highlighted by
427 the triterpenoid miliacin and its $\delta^{13}C$ signature, but also, to a minor extent, by the $\delta^{13}C$ signal
428 of 1-dotriacontanol.

429 *3.5. Extent of millet cropping inferred from stable carbon isotopes and ^{14}C dating*

430 The low contribution of lipids from millet to the *n*-alkyl lipid pool, as inferred from stable
431 carbon isotopes, could be explained on one hand by a limited contribution from millet biomass
432 to the SOM vs. that of C_3 plants (i.e. limited millet cropping). Such a situation might be
433 encountered if millet cropping were not quantitatively important in terms of surface cultivation
434 or of duration of cultivation. In this case, the molecular signature of *n*-alkyl lipids from millet
435 would be diluted with that from the predominating surrounding C_3 vegetation (natural or
436 cultivated in parallel with millet). Furthermore, the predominant C_3 vegetation that either
437 preceded or succeeded millet cropping might also be responsible for the observed isotopic
438 signature for the filling soils, a signature which was "sealed" within the silos after they were
439 abandoned.

440 In addition, irrespective of the importance of the initial contribution of millet biomass to SOM,
441 the stable carbon isotopic composition of straight chain lipids and miliacin within silo 1330 -
442 but probably also the other silos from the Iron Age - could be interpreted in terms of lipid
443 turnover associated with a vegetation change from a mixed C_3+C_4 vegetation to a pure C_3
444 vegetation cover in the light of the radiocarbon dating results. Indeed, there is a time difference
445 of several centuries between the age of miliacin (Bronze Age) and that of the silo (Iron Age) in

446 which miliacin was detected (Table 3). This difference implies that, following millet cultivation,
447 the soils underwent vegetation change before being trapped within the abandoned silo, this
448 vegetation being made up of C_3 plants (e.g. pasture or cereals like wheat, barley, ...) based on
449 the $\delta^{13}C$ values of the lipids and SOM (see above). The period during which the C_4 plus C_3
450 vegetation lasted cannot be determined, the radiocarbon age of miliacin corresponding to an
451 average age resulting from more ancient and more recent contributions, with unknown limits
452 for the beginning and end of this cereal crop. The progressive replacement of millet cropping
453 resulted in the "dilution" of the millet molecular and isotopic signatures by those of the newly
454 occupying C_3 plants. For each molecular structure considered, the replacement rate would
455 depend on one hand on the relative contribution of millet origin vs. C_3 plants and on the other
456 hand on the relative stability of each structure considered. For instance, miliacin, which has a
457 particularly stable structure due to the presence of the methoxy group at C-3, and which is not
458 biosynthesized by C_3 plants native to temperate regions (Bossard et al., 2013), would keep its
459 typical C_4 isotopic signature (i.e., no isotopic "dilution" given the absence of miliacin inputs
460 from a C_3 source). By contrast, in the case of straight chain lipids, the progressive degradation
461 of the C_4 source, together with the constant new input from straight chain lipids of C_3 origin,
462 would result in the progressive "dilution" of the molecular and isotopic signature of lipids of C_4
463 origin. Such a situation has some analogy with that reported by Mendez-Millan et al. (2014),
464 who investigated the evolution of the stable carbon isotopic composition of lipids from a soil
465 during a 30 yr chronosequence during which savannah (in this case dominated by C_4 plants)
466 was replaced by an eucalyptus plantation (a C_3 plant). Here, the molecular and isotopic
467 fingerprints from triterpenoid methyl ethers from savannah vegetation was only little affected
468 by the vegetation change, whereas the isotopic composition of the straight chain lipids was
469 progressively shifted towards more negative $\delta^{13}C$ values, as expected from such a vegetation
470 change. Based on stable carbon isotopes, it was notably determined that > 30 % of the *n*-C_{27}

alkane originated from the newly installed C_3 plant source after 30 yr of eucalyptus coverage. Conversely, in the case of a vegetation change from C_3 (wheat) to C_4 (maize) plants, the $\delta^{13}C$ values from soil constituents move towards less ^{13}C-depleted values (Lichtfouse et al., 1995).

3.6. Timing of millet cropping at the site of Obernai

Contrary to the protohistoric silos described above, the filling soil from silo 1817 (Mid-Neolithic, 4600-4300 BC) was devoid of miliacin, suggesting that millet was not cultivated at that time period. By contrast, structure 4564 (Roman Gaul period), corresponding to latrines, contained very high amounts of miliacin, having the same radiocarbon age (Table 3) as that of the structure. In this case, it seems that millet was consumed and likely cultivated locally at this period, in agreement with the literature (Reddé et al., 2005; Vandorpe and Wick, 2015).

The radiocarbon measurements allowed establishing that millet was cultivated during the Bronze Age and the Roman Gaul period at least, which makes sense in the light of the historical and archaeological data for the history of this cereal. In Alsace (NE France), where agricultural practices can be traced back down to ca. 4500 BC (Ruas and Marinval, 1991), very few archaeological studies report the detection of carpologic remains from millet during Protohistoric times, with only limited mention of its cultivation and consumption during the Iron Age (Wiethold, 2000; Bataille, 2014; Goude et al., 2015). This is also the case during the Roman period (Reddé et al., 2005; Vandorpe and Jacomet, 2011; Vandorpe and Wick, 2015), and the present study of the site of Obernai brings complementary information regarding millet cropping at the local and national scale during this period.

From an archaeological viewpoint, millet finds its origin in China where it was domesticated since the VIIth millenium BC (Laporte, 2001; Fuller, 2007; Lu et al., 2009). For instance, it has been recently shown that, in China, millet grains were fermented with other cereal grains to prepare beer (Wang et al., 2016). Later, millet culture began to spread through Asia and the

Middle East, before reaching Central Europe at the end of the Neolithic (Hunt et al., 2008). However, whereas in France wheat and barley were cultivated since the Neolithic (Ruas and Marinval, 1991; Martin et al., 2007), it is only during the Protohistoric times that cereal species became more diversified, and the first evidence from carpology of *P. miliaceum* culture can be dated back from the Early Bronze Age (ca. 1700 BC; Marinval, 1992, 1995). The Bronze and Iron Ages are clearly associated with intensified cultivation of this cereal in France. Millet grains were stored with their protecting envelopes (husks) for better preservation within the buried silos -like those found at Obernai - or in vases (Marinval, 1995). Following the conquest of Gaul, the Romans imported new varieties of cereals, mainly from the Mediterranean Basin, resulting in enhanced diversification of foodstuffs (Cabanis et al., 2015). This resulted in the progressive replacement of millet by other cereal species (e.g. rye), millet having been completely abandoned at the beginning of the Middle Age (Jacob et al., 2008a). Notwithstanding this, cultivation of millet lasted in Obernai at least until the end of the 2nd centuary AD – beginning of the 3rd centuary AD.

4. Conclusions

The archaeological site of Obernai (NE France) has provided the opportunity to investigate past local agricultural practices following unearthing of a series of protohistoric silos from the Bronze and Iron Ages. GC-MS analysis of the lipids preserved in the soils filling the silos has shown the presence of miliacin, a triterpenoid methyl ether strictly associated with the cereal *P. miliaceum* (broomcorn millet). However, the *n*-alkyl lipid assemblage co-detected with miliacin was associated to C3-plant sources for which no specific lipids were identified. The absence of a C4 isotopic signature for the *n*-alkyl lipids was probably caused by the turnover of the SOM induced by a change of vegetation cover. Radiocarbon dating of miliacin, SOM and lipid extracts indicated that millet cropping was established during the Bronze Age and during the Roman Gaul period. The study represents the first evidence of millet cultivation in Alsace

dating back to the Bronze Age, bringing a new perspective regarding agricultural practices and past diet in the East of France.

This study has also highlighted the potential of hollow archaeological structures like pits and silos to constitute "pedological traps" able to trap and archive soils surrounding the archaeological structures during their period of use or after abandoning. These filling soils have kept the molecular signatures from the various types of vegetation cover which developed on the surface soil horizons prior to being trapped in the structures, thereby potentially providing information about the past environment of archaeological sites in terms of vegetation cover or agricultural practices. This is notably the case for miliacin found in silos from the Iron Age in Obernai, attesting to millet cropping during the Bronze Age. The dating of lipids related to a given biological source and of specific biomarkers, together with their stable carbon isotopic composition, appeared to be critical for relating the molecular signatures to a specific chronological/historical context.

Acknowledgements

The INRAP (Institut National de Recherches Archéologiques Préventives) is thanked for providing the soil samples from the archaeological structures from Obernai, as is J. Jacob (Institut des Sciences de la Terre, Université d'Orléans, France) for providing an authentic miliacin standard and fresh material from broomcorn millet, and I. Antheaume and V. Grossi (University Claude Bernard Lyon I) for the bulk $\delta^{13}C$ analysis of SOM. B.C. thanks the French Ministère de l'Enseignement Supérieur et de la Recherche for a doctoral fellowship. Part of the radiocarbon data was financed through the project IDEX 2015 ARCHEOSOL (University of Strasbourg). L. Wacker is thanked for support via GIS AMS analysis at ETH Zurich.

References

543 Balesdent, J., Wagner, G.H., Mariotti, A., 1988. Soil organic matter turnover in long-term field
544 experiments as revealed by carbon-13 natural abundance. Soil Science Society of America
545 Journal 52, 118-124.

546 Ballentine, D.C., Macko, S.A., Turekian, V.C., 1998. Variability of stable carbon isotopic
547 compositions in individual fatty acids from combustion of C_4 and C_3 plants: implications for
548 biomass burning. Chemical Geology 152, 151-161.

549 Bataille, G., 2014. Eckbolsheim, Bas-Rhin. Parc d'activité – Les fouilles archéologiques
550 préalables à la construction des parkings et zones annexes du Zénith. Report, Vol. 2, INRAP
551 Grand Est Sud, Strasbourg.

552 Bi, X., Sheng, G., Liu, X., Li, C., Fu, J., 2005. Molecular and carbon and hydrogen isotopic
553 composition of *n*-alkanes in plant leaf waxes. Organic Geochemistry 36, 1405-1417.

554 Birkholz, A., Smittenberg, R.H., Hajdas, I., Wacker, L., Bernasconi, S.M., 2013. Isolation and
555 compound specific radiocarbon dating of terrigenous branched glycerol dialkyl glycerol
556 tetraethers (brGDGTs). Organic Geochemistry 60, 9-19.

557 Boëda, E., Connan, J., Dessort, D., Muhesen, S., Mercier, N., Valladas, H., Tisnérat, N., 1996.
558 Bitumen as a hafting material on Middle Palaeolithic artefacts. Nature 380, 336-338.

559 Bossard, N., Jacob, J., Le Milbeau, C., Sauze, J., Terwilliger, V., Poissonnier, B., Vergès, E.,
560 2013. Distribution of miliacin (olean-18-en-3β-ol methyl ether) and related compounds in
561 broomcorn millet (*Panicum miliaceum*) and other reputed sources: Implications for the use of
562 sedimentary miliacin as a tracer of millet. Organic Geochemistry 63, 48-55.

563 Buckley, S.A., Evershed, R.P., 2001. Organic chemistry of embalming agents in Pharaonic and
564 Graeco-Roman mummies. Nature 413, 837-841.

565 Bull, I.D., Simpson, I.A., Dockrill, S.J., Evershed, R.P., 1999. Organic geochemical evidence
566 for the origin of ancient anthropogenic soil deposits at Tofts Ness, Sanday, Orkney. Organic
567 Geochemistry 30, 535-556.

568 Bull I.D., Betancourt P.P., Evershed R.P., 2001. An organic geochemical investigation of the
569 practice of manuring at a Minoan site on Pseira Island, Crete. Geoarchaeology 16, 223-242.

570 Cabanis, M., Deberge, Y., Bouby, L., Hajnalovà, M., Marinval, P., Mennessier-Jouannet, C.,
571 Vermeulen, C., Vernet, G., 2015. Changes in crop cultivation during the last five centuries
572 before the Roman conquest: archaeobotanical investigation in the Clermont-Ferrand basin,
573 Massif Central, France. Archaeological and Anthropological Sciences, 1-16.

574 Charrié-Duhaut, A., Connan, J., Rouquette, N., Adam, P., Barbotin, C., de Rozières, M.-F.,
575 Tchapla, A., Albrecht, P., 2007. The canopic jars of Rameses II: real use revealed by molecular
576 study of organic residues. Journal of Archaeological Science 34, 957-967.

577 Charters, S., Evershed, R.P., Blinkhorn, P.W., Denham, V., 1995. Evidence for the mixing of
578 fats and waxes in archaeological ceramics. Archaeometry 37, 113-127.

579 Chikaraishi, Y., Naraoka, H., Poulson, S.R., 2004. Hydrogen and carbon isotopic fractionations
580 of lipid biosynthesis among terrestrial (C_3, C_4 and CAM) and aquatic plants. Phytochemistry
581 65, 1369-1381.

582 Chikaraishi, Y., Naraoka, H., 2006. Carbon and hydrogen isotope variation of plant biomarkers
583 in a plant-soil system. Chemical Geology 231, 190-202.

584 Chikaraishi, Y., Naraoka, H., 2007. δ13C and δD relationships among three *n*-alkyl compound
585 classes (*n*-alkanoic acid, *n*-alkane and *n*-alkanol) of terrestrial higher plants. Organic
586 Geichemistry 38, 198-215.

587 Christl, M., Vockenhuber, C., Kubik, P.W., Wacker, L., Lachner, J., Alfimov, V., Synal, H.-
588 A., 2013. The ETH Zurich AMS facilities: performance parameters and reference materials.
589 Nuclear Instruments and Methods in Physics Research B 294, 29-38.

590 Collister, J.W., Rieley, G., Stern, B., Eglinton, G., Fry, B., 1994. Compound-specific $\delta^{13}C$
591 analyses of leaf lipids from plants with differing carbon dioxide metabolisms. Organic
592 Geochemistry 21, 619-627.

593 Condamin, J., Formenti, F., Metais, M.O., Michel, M., Blond, P., 1976. The application of gas
594 chromatography to the tracing of oil in ancient amphorae. Archaeometry 18, 195-201.

595 Connan, J., 1999. Use and trade of bitumen in antiquity and prehistory: molecular archaeology
596 reveals secrets of past civilizations. Philosophical Transactions of the Royal Society B:
597 Biological Sciences 354, 33-50.

598 Courel, B., Schaeffer, P., Adam, P., Ertlen, D., Schwartz, D., Bernasconi, S.M., Hajdas, I., 2015.
599 Analyse, isolement et datation au ^{14}C de lipides dans les sols. L'exemple des tétraéthers de
600 diglycérol. In : Poulenard, J., Rossi, M. (Eds.), Sols et Matières Organiques: Mémoires et
601 Héritages. EDYTEM. Université de Savoie, Le Bourget-du Lac, pp 57-68.

602 Egli, M., Gristina, L., Wiesenberg, G.L.B., Civantos, J.M.M., Rotolo, A., Novara A., Brandová,
603 D., Raimondi, S., 2013. From pedologic indications to archaeological reconstruction:
604 deciphering land use in the Islamic period in the Baida district (north-western Sicily). Journal
605 of Archaeological Science 40, 2670-2685.

606 Eglinton, G., Logan, G.A., 1991. Molecular preservation. Philosophical Transactions of the
607 Royal Society B: Biological Sciences 333, 315-328.

608 Ertlen, D., Féliu, C., Michler, M., Schneider-Schwien, N., Schneikert, F., Thomas, Y., Braguier,
609 S., Minni, D., Veber, C., 2013. Les structures de type « fente » dans le Kochersberg (Alsace):

610 un programme de recherche en cours de développement. Revue archéologique de l'Est,
611 Supplément 33, 213-227.

612 Ertlen, D., Schwartz, D., Brunet, D., Trendel, J.-M., Adam, P., Schaeffer, P., 2015. Qualitative
613 near infrared spectroscopy, a new tool to recognize past vegetation signature in soil organic
614 matter. Soil Biology & Biochemistry 82, 127-134.

615 Evershed, R.P., Heron, C., Goad, L.J., 1991. Epicuticular wax components preserved in
616 potsherds as chemical indicators of leafy vegetables in ancient diets. Antiquity 65, 540-544.

617 Fuller, D.Q., 2007. Contrasting patterns in crop domestication and domestication rates: recent
618 archaeobotanical insights from the Old World. Annals of Botany 100, 903-924.

619 Gierga, M., Hajdas, I., van Raden, U.J., Gilli, A., Wacker, L., Sturm, M., Bernasconi, S.M.,
620 Smittenberg, R.H., 2016. Long-stored soil carbon released by prehistoric land use: evidence
621 from compound-specific radiocarbon analysis on Soppensee lake sediments. Quaternary
622 Science Reviews 144, 123-131.

623 Goude, G., Balasescu, A., Réveillas, H., Thomas, Y., Lefranc, P., 2015. Diet variability and
624 stable isotope analyses: looking for variables within the Late Neolithic and Iron Age human
625 groups from Gougenheim site and surrounding areas (Alsace, France). International Journal of
626 Osteoarchaeology 25, 988-996.

627 Hengtrakul, P. Lorenz, K., Mathias, M., 1991. Alkylresorcinol homologs in cereal grains.
628 Journal of Food Composition and Analysis 4, 52-57.

629 Huang, Y., Bol, R., Harkness, D.D., Ineson, P., Eglinton, G., 1996. Post-glacial variations in
630 distributions, ^{13}C and ^{14}C contents of aliphatic hydrocarbons and bulk organic matter in three
631 types of British acid upland soils. Organic Geochemistry 24, 273-287.

632 Hunt, H.V., Linden, M.V., Liu, X., Motuzaite-Matuzeviciute, G., Colledge, S., Jones, M.K.,
633 2008. Millets across Eurasia: chronology and context of early records of the genera *Panicum*
634 and *Setaria* from archaeological sites in the Old World. Vegetation History and Archaeobotany
635 17 (Suppl 1), S5-S18.

636 Ingalls, A.E., Pearson, A., 2005. Ten years of compound-specific radiocarbon analysis.
637 Oceanography 18, 18-31.

638 Jacob, J., Disnar, J.-R., Boussafir, M., Albuquerque, A.L.S., Sifeddine, A., Turcq, B., 2005.
639 Pentacyclic triterpene methyl ethers in recent lacustrine sediments (Lagoa do Caçó, Brazil).
640 Organic Geochemistry 36, 449-461.

641 Jacob, J., Disnar, J.-R., Arnaud, F., Chapron, E., Debret, M., Lallier-Vergès, E., Desmet, M.,
642 Revel-Rolland, M., 2008a. Millet cultivation history in the French Alps as evidenced by a
643 sedimentary molecule. Journal of Archaeological Science 35, 814-820.

644 Jacob, J., Disnar, J.-R., Bardoux, G., 2008b. Carbon isotope evidence for sedimentary miliacin
645 as a tracer of *Panicum miliaceum* (broomcorn millet) in the sediments of Lake le Bourget
646 (French Alps). Organic Geochemistry 39, 1077-1080.

647 Koch, P.L., Fogel, M.L., Tuross, N., 1994. Tracing the diets of fossil animals using stable
648 isotopes. In: Lajtha, K., Michener, R.H. (Eds.), Stable Isotopes in Ecology and Environmental
649 Science, 1st Edition. Blackwell Scientific Publications, pp. 63-92.

650 Kögel-Knabner, I., 2002. The macromolecular organic composition of plant and microbial
651 residues as inputs to soil organic matter. Soil Biology & Biochemistry 34, 139-162.

652 Laporte, L., 2001. Guilaine, (J.), Dir. – Premiers paysans du monde, naissance des agricultures.
653 Séminaire du Collège de France. Revue Archéologique de l'Ouest 18, 240-242.

Lavrieux, M., Jacob, J., Le Milbeau, C., Zocatelli, R., Masuda, K., Bréheret, J.-G., Disnar, J.-R., 2011. Occurrence of triterpenyl acetates in soil and their potential as chemotaxonomical markers of *Asteraceae*. Organic Geochemistry 42, 1315-1323.

Lavrieux, M., Bréheret, J.-G., Disnar, J.-R., Jacob, J., Le Milbeau, C., Zocatelli, R., 2012. Preservation of an ancient grassland biomarker signature in a forest soil from the French Massif Central. Organic Geochemistry 51, 1-10.

Lavrieux, M., Jacob, J., Disnar, J.-R., Bréheret, J.-G., Le Milbeau, C., Miras, Y., Andrieu-Ponel, V., 2013. Sedimentary cannabinol tracks the history of hemp retting. Geology 41, 751-754.

Lichtfouse, E., Dou, S., Houot, S., Barriuso, E., 1995. Isotope evidence for soil organic carbon pools with distinct turnover rate -II. Humic substances. Organic Geochemistry 23, 845-847.

Lichtfouse, E., Bardoux, G., Mariotti, A., Balesdent, J., Ballentine, D.C., Macko, S.A., 1997. Molecular, ^{13}C, and ^{14}C evidence for the allochthonous and ancient origin of C_{16}-C_{18} *n*-alkanes in modern soils. Geochimica et Cosmochimica Acta 61, 1891-1898.

Lorenz, K., Lal, R., Preston, C.M., Nierop, K.G.J., 2007. Strengthening the soil organic carbon pool by increasing contributions from recalcitrant aliphatic bio(macro)molecules. Geoderma 142, 1-10.

Lu, H., Zhang J., Liu, K.-B., Wu, N., Li, Y., Zhou, K., Ye, M., Zhang, T., Zhang, H., Yang, X., Shen, L., Xu, D., Li, Q., 2009. Earliest domestication of common millet (*Panicum miliaceum*) in East Asia extended to 10,000 years ago. Proceedings of the National Academy of Sciences USA 106, 7367-7372.

Marinval, P., 1992. Archaeobotanical data on millets (*Panicum miliaceum* and *Setaria italica*) in France. Review of Palaeobotany and Palynology 73, 259-270.

676 Marinval, P., 1995. Données carpologiques françaises sur les Millets (*Panicum miliaceum* L. et
677 *Setaria italica* (L.) Beauv.) de la Protohistoire au Moyen Age. In: Hörandner, E. (Ed.), Millet:
678 Actes du Congrès d'Aizenay, 18-19 août 1990. Peter Lang, Frankfurt, pp. 31-61.

679 Mariotti, A., Peterschmitt, E., 1994. Forest savanna ecotone dynamics in India as revealed by
680 carbon isotope ratios of soil organic matter. Oecologia 97, 475-480.

681 Martin, L., Thiébault, S., Rey, P.-J., 2007. Production et consommation végétale durant la
682 Préhistoire récente: études archéobotaniques de quelques sites des Alpes occidentales. In:
683 Boëtsch, G., Hubert, A (Eds.), Alimentation et Montagne, Actes de la 6ème Université
684 Européenne d'Eté « Anthropologie des Populations Alpines », Gap, France. Editions des
685 Hautes-Alpes, Gap, pp. 11-24.

686 Mendez-Millan, M., Nguyen Tu, T.T., Balesdent, J., Derenne, S., Derrien, D., Egasse, C.,
687 Thongo M'Bou, A., Zeller, B., Hatté, C., 2014. Compound-specific ^{13}C and ^{14}C measurements
688 improve the understanding of soil organic matter dynamics. Biogeochemistry 118, 205-223.

689 Mollenhauer, G., Rethemeyer, J., 2009. Compound-specific radiocarbon analysis - analytical
690 challenges and applications. IOP Conferences Series: Earth and Environmental Science 5,
691 012006.

692 Motuzaite-Matuzeviciute, G., Jacob, J., Telizhenko, S., Jones, M.K., 2016. Miliacin in
693 palaeosols from an Early Iron Age in Ukraine reveals *in situ* cultivation of broomcorn millet.
694 Archaeological and Anthropological Sciences 8, 43-50.

695 Ohmoto, T., Ikuse, M., Natori, S., 1970. Triterpenoids of the *Gramineae*. Phytochemistry 9,
696 2137-2148.

697 O'Leary, M.H., 1988. Carbon isotopes in photosynthesis. BioScience 38, 328-336.

698 Pessenda, L.C.R., Gomes, B.M., Aravena, R., Ribeiro, A.S., Boulet, R., Gouveia, S.E.M., 1998.
699 The carbon isotope record in soils along a forest-cerrado ecosystem transect: implications for
700 vegetation changes in the Rondonia state, southwestern Brazilian Amazon region. The
701 Holocene 8, 599-603.

702 Quénéa, K., Largeau, C., Derenne, S., Spaccini, R., Bardoux, G., Mariotti, A., 2006. Molecular
703 and isotopic study of lipids in particle size fractions of a sandy cultivated soil (Cestas cultivation
704 sequence, southwest France): Sources, degradation, and comparison with Cestas forest soil.
705 Organic Geochemistry 37, 20-44.

706 Reddé, M., Nuber, H.U., Jacomet, S., Schibler, J., Schucany, C., Schwarz, P.-A., Seitz, G.,
707 Ginella, F., Joly, M., Plouin, S., Hüster Plogmann, H., Petit, C., Popovitch, L., Schlumbaum,
708 A., Vandorpe, P., Viroulet, B., Wick, L., Wolf, J.-J., Gissinger, B., Ollive, V., Pellissier, J.,
709 2005. Oedenburg. Une agglomération d'époque romaine sur le Rhin supérieur: fouilles
710 françaises, allemandes et suisses à Biesheim-Kunheim (Haut-Rhin). Gallia 62, 215-277.

711 Reimer, P.J., Bard, E., Bayliss, A., Beck, J.W., Blackwell, P.G., Ramsey, C.B., Buck, C.E.,
712 Cheng, H., Edwards, R.L., Friedrich, M., Grootes, P.M., Guilderson, T.P., Haflidason, H.,
713 Hajdas, I., Hatté, C., Heaton, T.J., Hoffmann, D.L., Hogg, A.G., Hughen, K.A., Kaiser, K.F.,
714 Kromer, B., Manning, S.W., Niu, M., Reimer, R.W., Richards, D.A., Scott, E.M., Southon, J.R.,
715 Staff, R.A., Turney, C.S.M., van der Plicht, J., 2013. IntCal13 and Marine13 radiocarbon age
716 calibration curves 0-50,000 years cal BP. Radiocarbon 55, 1869-1887.

717 Rethemeyer, J., Kramer, C., Gleixner, G., Wiesenberg, G.L.B., Schwark, L., Andersen, N.,
718 Nadeau, M.-J., Grootes, P.M., 2004. Complexity of soil organic matter: AMS ^{14}C analysis of
719 soil lipid fractions and individual compounds. Radiocarbon 46, 465-473.

720 Rethemeyer, J., Kramer, C., Gleixner, G., John, B., Yamashita, T., Flessa, H., Andersen, N.,
721 Nadeau, M.-J., Grootes, P.M., 2005. Transformation of organic matter in agricultural soils:
722 radiocarbon concentration versus soil depth. Geoderma 128, 94-105.

723 Rieley, G., 1994. Derivatization of organic compounds prior to gas chromatographic-
724 combustion-isotope ratio mass spectrometric analysis: identification of isotope fractionation
725 processes. Analyst 119, 915-919.

726 Ross, A.B., Shepherd, M.J., Schüpphaus, M., Sinclair, V., Alfaro, B., Kamal-Eldin, A., Åman,
727 P., 2003. Alkylresorcinols in cereal and cereal products. Journal of Agricultural and Food
728 Chemistry 51, 4111-4118.

729 Ross, A.B., Åman, P., Andersson, R., Kamal-Eldin, A., 2004. Chromatographic analysis of
730 alkylresorcinols and their metabolites. Journal of Chromatography A 1054, 157-164.

731 Ruas, M.-P., Marinval, P., 1991. Alimentation végétale et agriculture d'après les semences
732 archéologiques (de 9000 av. J.-C. au XV^{e} siècle). In: Guilaine, J. (Ed), Pour une Archéologie
733 Agraire. Armand Colin, pp. 409-439.

734 Ruff, M., Wacker, L., Gäggeler, H.W., Suter, M., Synal, H.-A., Szidat, S., 2007. A gas ion
735 source for radiocarbon measurements at 200 kV. Radiocarbon 49, 307-314.

736 Ruff, M., Fahrni, S., Gäggeler, H.W., Hajdas, I., Suter, M., Synal, H.-A., Szidat, S., Wacker,
737 L., 2010. On-line radiocarbon measurements of small samples using elemental analyzer and
738 MICADAS gas ion source. Radiocarbon 52, 1645-1656.

739 Schmidt, M.W.I., Torn, M.S., Abiven, S., Dittmar, T., Guggenberger, G., Janssens, I.A., Kleber,
740 M., Kögel-Knabner, I., Lehmann, J., Manning, D.A.C., Nannipieri, P., Rasse, D.P., Weiner, S.,
741 Trumbore, S.E., 2011. Persistence of soil organic matter as an ecosystem property. Nature 478,
742 49-56.

743 Schnell, G., Schaeffer, P., Tardivon, H., Motsch, E., Connan, J., Ertlen, D., Schwartz, D.,
744 Schneider, N., Adam, P., 2014. Contrasting diagenetic pathways of higher plant triterpenoids
745 in buried wood as a function of tree species. Organic Geochemistry 66, 107-124.

746 Schwartz, D., 1991. Intérêt de la mesure du $\delta^{13}C$ des sols en milieu naturel équatorial pour la
747 connaissance des aspects pédologiques et écologiques des relations savane-forêt. Cahiers
748 ORSTOM, Série Pédologie 26, 327-341.

749 Schwartz, D., 2012. Les temps du sol : interprétations temporelles de l'archivage pédologique
750 dans les approches paléoenvironnementalistes et géoarchéologiques. Étude & Gestion des Sols
751 19, 51-65.

752 Seitz, L.M., 1992. Identification of 5-(2-oxoalkyl)resorcinols and 5-(2-oxoalkenyl)resorcinols
753 in wheat and rye grains. Journal of Agricultural and Food Chemistry 40, 1541-1546.

754 Sistiaga, A., Mallol C., Galván, B., Summons, R.E., 2014. The Neanderthal meal: a new
755 perspective using faecal biomarkers. PLOS ONE 9, e101045.

756 Stuiver, M., Polach, H.A., 1977. Discussion: reporting of ^{14}C data. Radiocarbon 19, 355–363.

757 Synal, H.-A., Stocker, M., Suter, M., 2007. MICADAS: a new compact radiocarbon AMS
758 system. Nuclear Instruments and Methods in Physics Research B 259, 7-13.

759 Trendel, J.M., Schaeffer, P., Adam, P., Ertlen, D., Schwartz, D., 2010. Molecular
760 characterisation of soil surface horizons with different vegetation in the Vosges Massif (France).
761 Organic Geochemistry 41, 1036-1039.

762 Tulloch, A.P., 1982. Epicuticular waxes of *Panicum miliaceum*, *Panicum texanum* and *Setaria*
763 *italica*. Phytochemistry 21, 2251-2255.

van Bergen, P.F., Bull, I.D., Poulton, P.R., Evershed, R.P., 1997. Organic geochemical studies of soils from the Rothamsted classical experiments – I. Total lipid extracts, solvent insoluble residues and humic acids from Broadbalk Wilderness. Organic Geochemistry 26, 117-135.

van der Merwe, N.J., Vogel, J.C., 1983. Recent carbon isotope research and its implications for African archaeology. African Archaeological Review 1, 35-56.

Vandorpe, P., Jacomet, S., 2011. Plant economy and environment. In: Vandorpe, P., Plant macro remains from the 1st and 2nd Cent. A.D. in Roman Oedenburg/Biesheim-Kunheim (F). Methodological aspects and insights into local nutrition, agricultural practices, import and the natural environment. Habilitation Thesis, University of Basel, Switzerland.

Vandorpe, P., Wick, L., 2015. Food plants in anthropogenic sediments as represented in pollen and macrofossil spectra: a case study on waterlogged Roman sediments from Switzerland and Alsace, France. Vegetation History and Archaeobotany 24, 135-142.

Wacker, L., Němec, M., Bourquin, J., 2010a. A revolutionary graphitisation system: fully automated, compact and simple. Nuclear Instruments and Methods in Physics Research B 268, 931-934.

Wacker, L., Bonani, G., Friedrich, M., Hajdas, I., Němec, M., Ruff, M., Suter, M., Synal, H.-A., Vockenhuber, C., 2010b. MICADAS: routine and high-precision radiocarbon dating. Radiocarbon 52, 252-262.

Wang, J., Liu, L., Ball, T., Yu, L., Li, Y., Xing, F., 2016. Revealing a 5,000-y-old beer recipe in China. Proceedings of the National Academy of Sciences USA 113, 6444-6448.

Wiesenberg, G.L.B., Schwarzbauer, J., Schmidt, M.W.I., Schwark, L., 2004. Source and turnover of organic matter in agricultural soils derived from *n*-alkane/*n*-carboxylic acid compositions and C-isotope signatures. Organic Geochemistry 35, 1371-1393.

787 Wiethold, J., 2000. Macro-restes végétaux imbibés et carbonisés du premier âge du Fer
788 provenant de fouille sauvetage de chantier 'les résidences du vignoble' à Hattstatt-
789 'Ziegelscheuer' (Haut-Rhin). In: Dumont, A., Treffort, J.M. (Eds), Hattstatt « Ziegelsheuer »
790 « Les résidences du vignoble », 68 – Haut-Rhin, Puits à eau protohistoriques (Bronze Ancien
791 et Hattstatt C). Afan Grand-Est, Strasbourg.

792 Winata, A., Lorenz, K., 1997. Effects of fermentation and baking of whole wheat and whole
793 rye sourdough breads on cereal alkylresorcinols. Cereal Chemistry 74, 284-287.

794

795 **Figure captions:**

796 **Fig. 1**. Photos and cross-sections of selected archaeological structures unearthed at Obernai
797 (Alsace, NE France); a, Silo 1330; b, Gaulish pit; c, Roman Gaul latrines; AL, Archaeological
798 layer; LS, loess substrate. Photos and drawings by Clément Féliu (INRAP).

799 **Fig. 2.** Gas chromatograms (GC-MS, conditions B) of the apolar fraction from the lipid extract
800 from (a) silo 1330.AL2, (b) silo 1330.LS, (c) pit 1001.AL23 and (d) latrines 4564.AL8 (Obernai,
801 NE France). Carboxylic acids are analysed as methyl esters and alcohols as acetates. Numbers
802 refer to structures in Appendix A.

803 **Fig. 3.** Amount of miliacin (µg/g soil) in the soils collected within the archaeological layers of
804 the silos (AL) and the Gaulish pit as well as in their respective loess substrates (LS).

805 **Fig. 4.** Graphical representation of ^{14}C age cal. BP obtained for isolated miliacin samples (in
806 blue), lipid extracts (in red), soil organic matter (in grey), carbonized grains of millet (in green)
807 in respect to the age of the archaeological structures determined by ceramology. The non-
808 calibrated ^{14}C ages are marked with a black cross (for standard deviation, see Table 3).

809

810

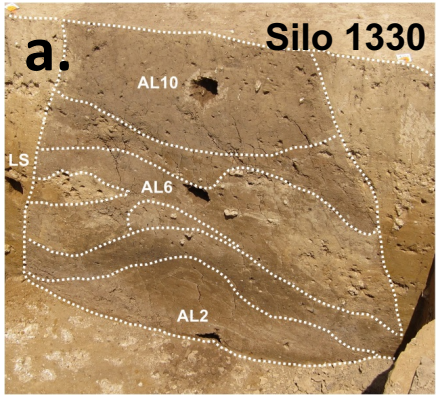
a.
Silo 1330
AL10
LS
AL6
AL2

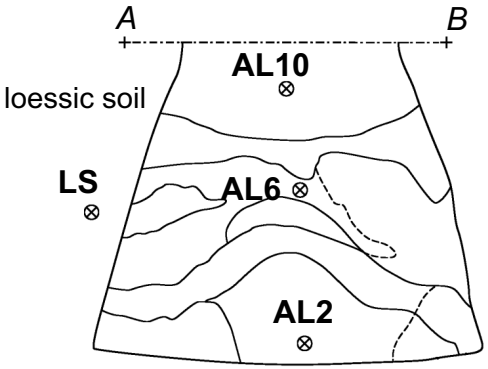
A
B
AL10
loessic soil
LS
AL6
AL2

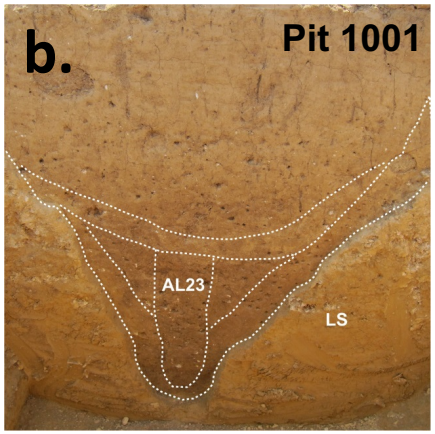
b.
Pit 1001
AL23
LS

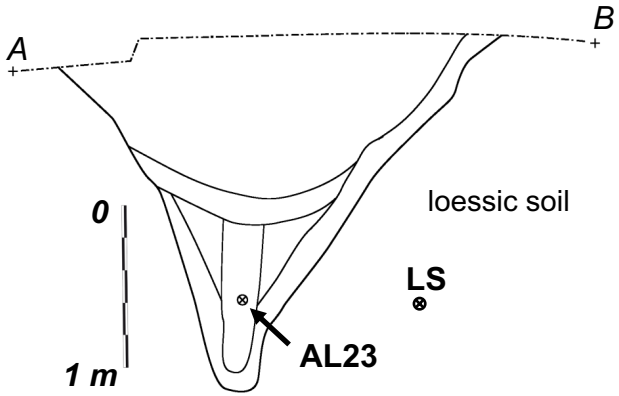
A
B
loessic soil
0
LS
AL23
1 m

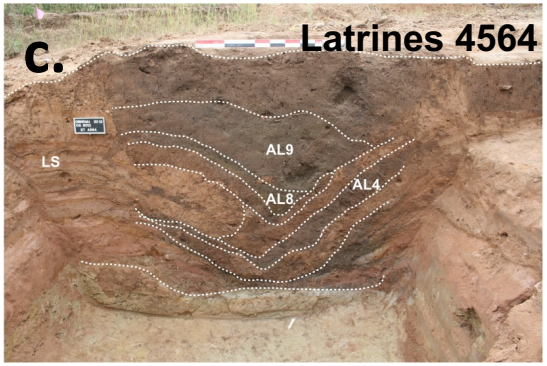
c.
Latrines 4564
LS
AL9
AL8
AL4

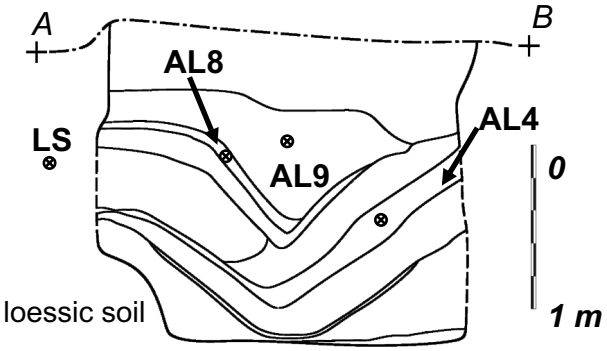
A
B
AL8
LS
AL4
AL9
0
loessic soil
1 m

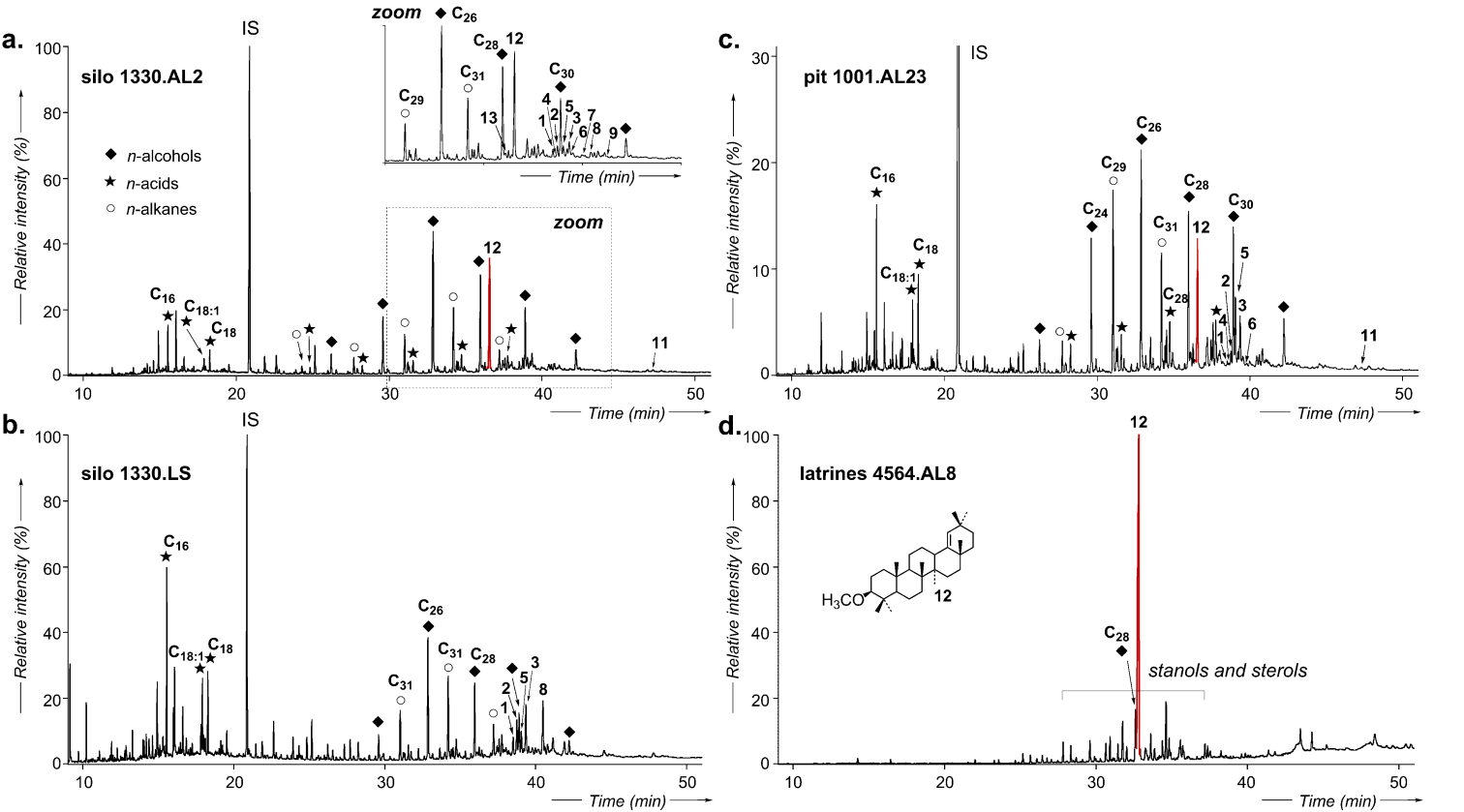
a.
silo 1330.AL2
IS
zoom
C26
C28
12
C31
C30
C29
4
2
5
1
3
7
13
6
8
9
Time (min)
zoom
12
C16
C18:1
C18
11
n-alcohols
n-acids
n-alkanes
Relative intensity (%)
Time (min)
b.
silo 1330.LS
IS
C16
C26
C18:1
C18
C31
C28
5
3
2
8
1
Relative intensity (%)
Time (min)
c.
pit 1001.AL23
IS
C26
C16
C29
C28
C24
C30
C31
12
5
C18
C18:1
2
C28
3
4
1
6
11
Relative intensity (%)
Time (min)
d.
latrines 4564.AL8
12
H3CO
12
C28
stanols and sterols
Relative intensity (%)
Time (min)

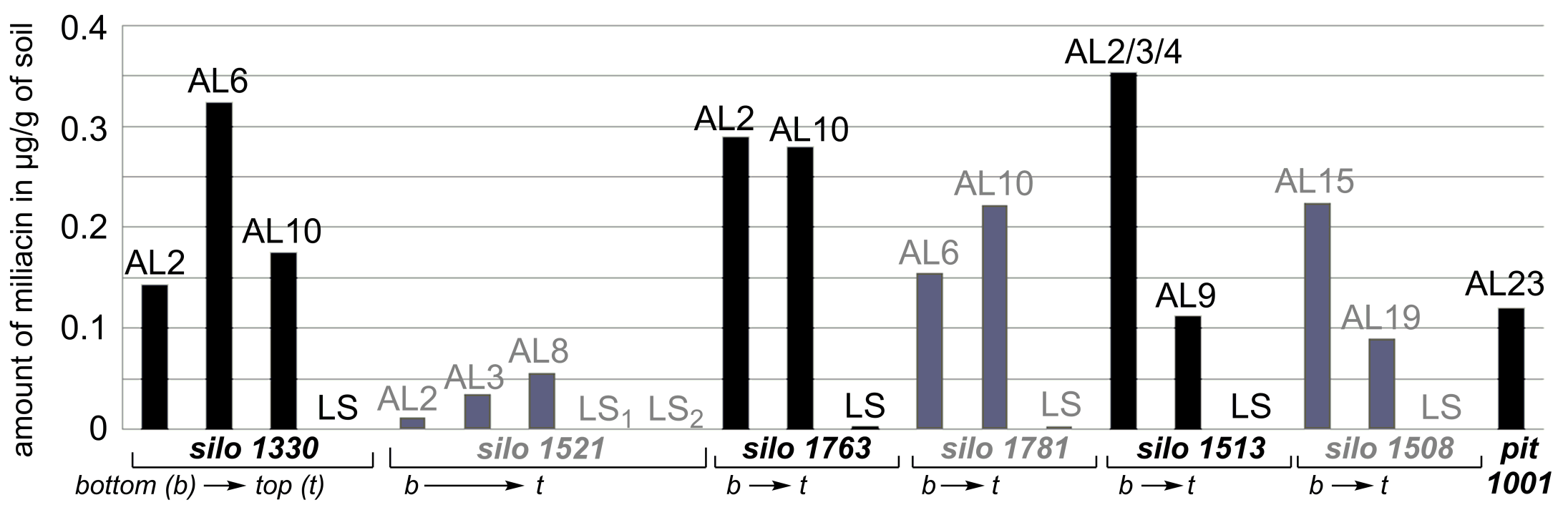
amount of miliacin in µg/g of soil
0.4
0.3
0.2
0.1
0
AL2
AL6
AL10
LS
AL2
AL3
AL8
LS1
LS2
AL2
AL10
LS
AL6
AL10
LS
AL2/3/4
AL9
LS
AL15
AL19
LS
AL23
silo 1330
silo 1521
silo 1763
silo 1781
silo 1513
silo 1508
pit 1001
bottom (b) → top (t)
b → t
b → t
b → t
b → t
b → t

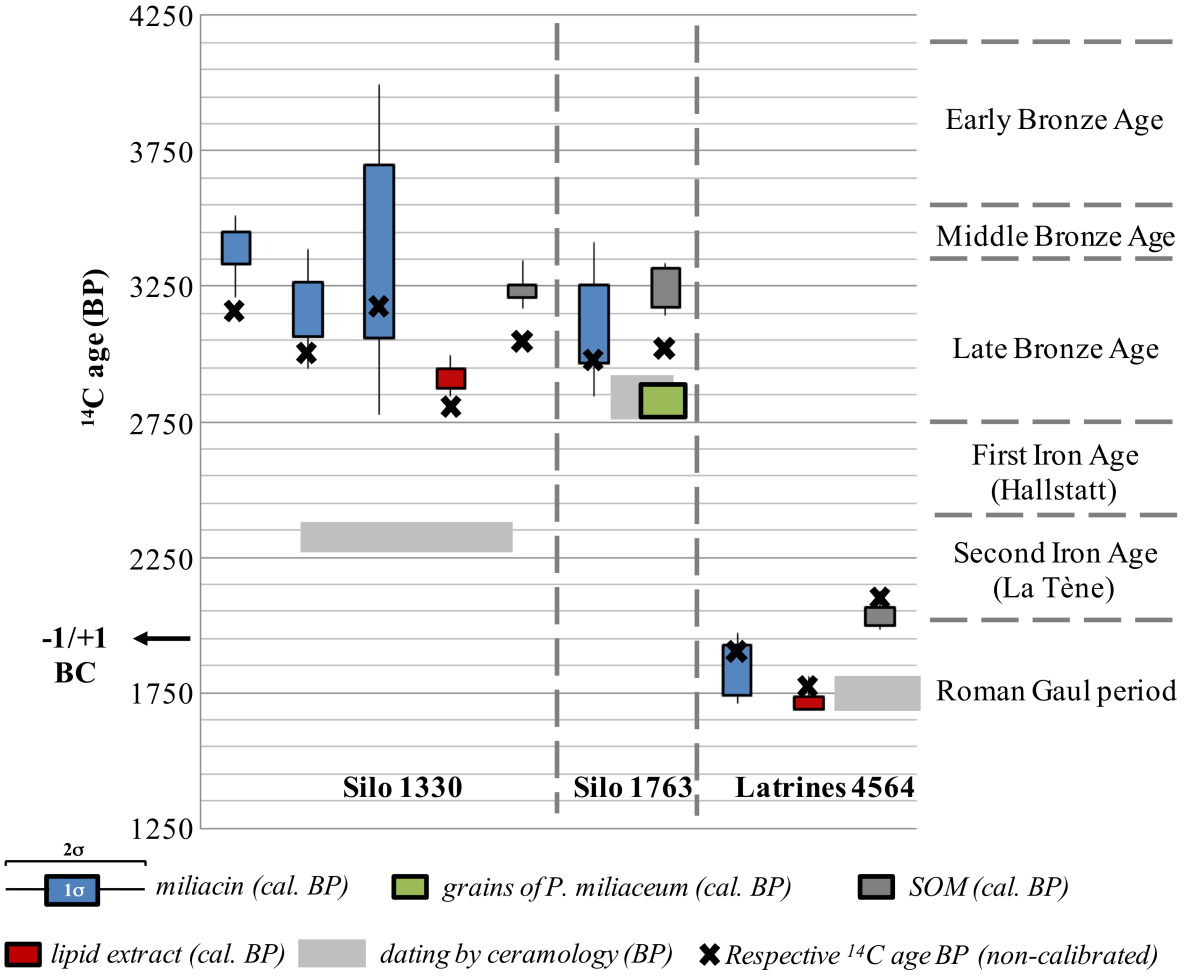
4250
3750
3250
2750
2250
1750
1250
14C age (BP)
-1/+1
BC
Early Bronze Age
Middle Bronze Age
Late Bronze Age
First Iron Age
(Hallstatt)
Second Iron Age
(La Tène)
Roman Gaul period
Silo 1330
Silo 1763
Latrines 4564
2σ
1σ
miliacin (cal. BP)
grains of P. miliaceum (cal. BP)
SOM (cal. BP)
lipid extract (cal. BP)
dating by ceramology (BP)
Respective 14C age BP (non-calibrated)

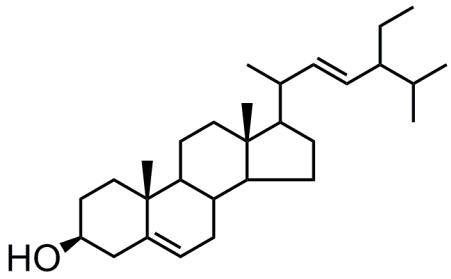

1

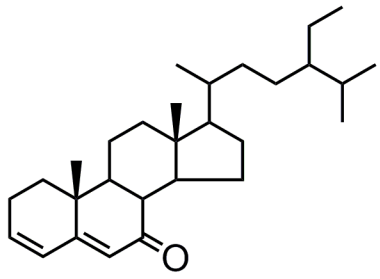

2

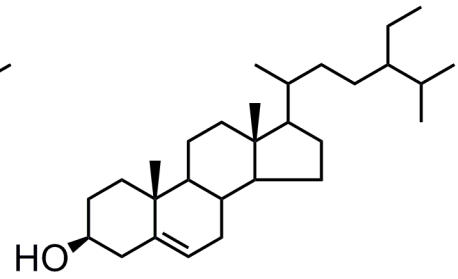

3

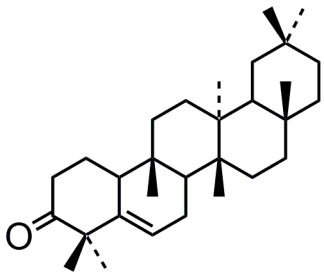

4

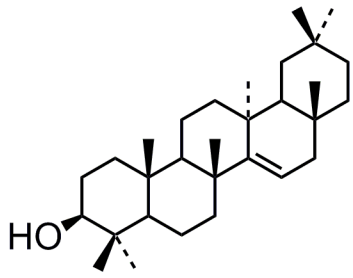

5

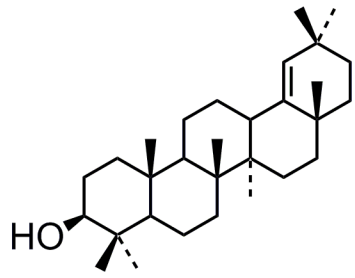

6

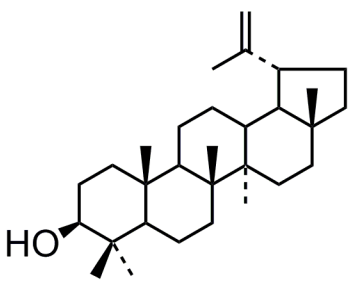

7

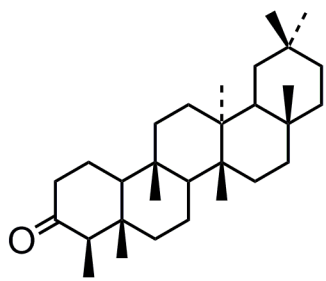

8

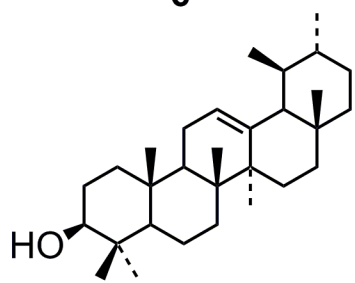

9

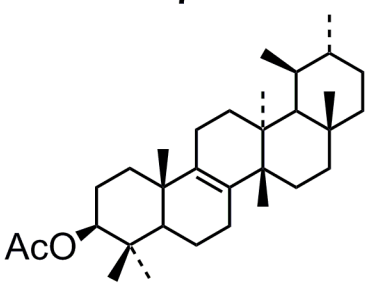

10

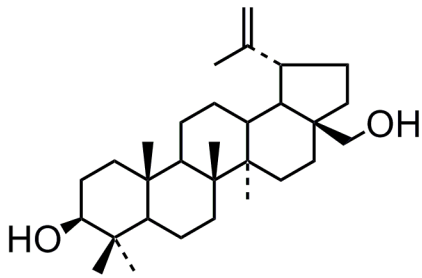

11

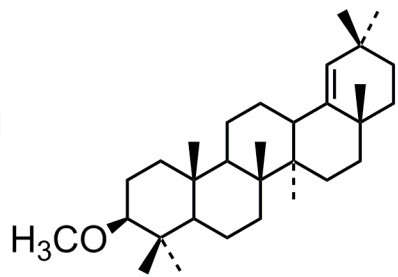

12

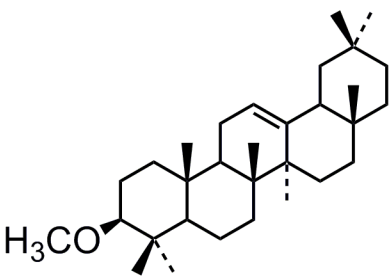

13

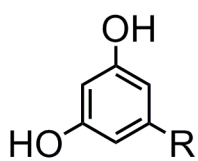

alkylresorcinols

R: Alkyl chains
(odd carbon numbered,
typically C_{15}-C_{25})

Table 1

Archaeological structures sampled for lipid analysis and age of the structures determined from ceramology.

	Archaeological age	Historical period	Sampling level[a]
		Silos	
1330	400-260 BC	La Tène B	AL2, AL6, AL10, LS
1508	400-260 BC	La Tène B	AL15, AL19, LS
1513	400-260 BC	La Tène B	AL2/3/4, AL9, LS
1521	150-30 BC	La Tène D	AL2, AL3, AL8, LS1, LS2
1763	950-800 BC	Late Bronze Age	AL2, AL10, LS
1781	400-260 BC	La Tène B	AL6, AL10, LS
1817	4600-4300 BC	Neolithic period	AL3, AL8, AL9, LS1, LS2
		Latrines	
4564	End of 2nd c. AD – beginning of the 3rd c. AD	Roman period	AL4, AL8, AL9, LS
		Gaulish pit	
1001	150-30 BC	La Tène D	AL23, LS

[a] Location within the archaeological layers (AL) of the structures and in the loess substrates (LS) are illustrated in Fig. 1 and Fig. S1 (Supplementary data).

Table 2

Stable carbon isotopic composition ($\delta^{13}C$, ‰ vs. VPDB) and standard deviation ($\pm\sigma$) of individual lipids from selected silo samples (AL) and one loess substrate sample (LS ; n.d., not determined).

$\delta^{13}C$	1330.AL2	1508.AL15	1508.LS	1513.AL9	1521.AL8	1817.AL3	1763.AL2
				n-Alkanes			
C_{25}	-31.8 (± 0.7)	-32.1 (± 0.5)	-33.1 (± 0.4)	-32.5 (± 0.2)	-31.8 (± 0.4)	-31.8 (± 0.5)	-29.9 (± 0.5)
C_{27}	-31.5 (± 0.6)	-31.9 (± 0.2)	-32.1 (± 0.3)	-31.9 (± 0.2)	-31.7 (± 0.4)	-32.5 (± 0.1)	-30.4 (± 0.2)
C_{29}	-33.5 (± 0.5)	-34.0 (± 0.3)	-33.6 (± 0.1)	-33.9 (± 0.1)	-33.5 (± 0.3)	-33.5 (± 0.2)	-32.5 (± 0.2)
C_{31}	-34.7 (± 0.2)	-34.5 (± 0.2)	-34.2 (± 0.1)	-35.4 (± 0.5)	-34.1 (± 0.5)	-34.3 (± 0.2)	-33.4 (± 0.2)
C_{33}	-35.5 (± 0.3)	-33.0 (± 0.1)	-33.5 (± 0.3)	-33.9 (± 0.2)	-34.5 (± 1.0)	-34.5 (± 0.3)	-32.9 (± 0.4)
				n-Alcohols[a]			
C_{22}	-33.6 (± 0.6)	-33.8 (± 0.4)	-33.6 (± 0.3)	-32.6 (± 0.2)	-33.6 (± 0.4)	-33.8 (± 0.4)	-33.4 (± 0.3)
C_{24}	-33.6 (± 0.3)	-33.9 (± 0.1)	-34.3 (± 0.2)	-33.7 (± 0.4)	-32.8 (± 0.1)	-33.4 (± 0.4)	-34.8 (± 0.2)
C_{26}	-35.9 (± 0.2)	-36.2 (± 0.1)	-35.4 (± 0.1)	-36.2 (± 0.2)	-36.1 (± 0.2)	-34.9 (± 0.2)	-36.8 (± 0.2)
C_{28}	-36.2 (± 0.2)	-36.1 (± 0.1)	-35.6 (± 0.1)	-36.1 (± 0.2)	-35.8 (±0.2)	-35.3 (± 0.6)	-35.5 (± 0.1)
C_{30}	-34.6 (± 0.5)	-34.9 (± 0.2)	-35.6 (± 0.5)	-35.1 (± 0.3)	-35.8 (± 0.2)	-35.3 (± 0.3)	n.d.
C_{32}	-33.6 (± 0.7)	-31.4 (± 0.2)	-32.6 (± 0.4)	-33.1 (± 0.4)	-32.7 (± 0.1)	-35.4 (±0.2)	-33.2 (± 0.4)

$\delta^{13}C$	1508.AL15	1513.AL9	1521.AL8	1763.AL2
		n-Acids[a]		
C_{20}	-32.6 (± 0.4)	n.d.	n.d.	-31.6 (± 0.2)
C_{22}	-33.8 (± 0.2)	n.d.	n.d.	-31.7 (± 0.2)
C_{24}	-32.8 (± 0.2)	n.d.	n.d.	-32.8 (± 0.3)
C_{26}	-33.7 (± 0.4)	n.d.	n.d.	-34.7 (± 0.4)
C_{28}	-34.6 (± 0.2)	n.d.	n.d.	-36.3 (± 0.4)
C_{30}	n.d.	n.d.	n.d.	-36.2 (± 0.4)
C_{32}	-34.9 (± 0.7)	n.d.	n.d.	-37.0 (± 0.5)
		Miliacin (**12**)		
	-21.6 (± 0.1)	-21.5 (±0.1)	-21.3 (±0.3)	n.d.

[a] Values corrected for derivatization agent [$Si(CH_3)_3$ and CH_3 for the *n*-alcohols and *n*-acids, respectively].

Table 3

^{14}C age (in BP[a] and cal. BC/AD[b]) of soil organic matter (SOM), lipid extract (LE) and isolated miliacin (**12**) from selected soil samples.

Sample	Amount of soil	SOM (decarbonated soil) Age ^{14}C BP[a] (±1σ)	Cal. age ^{14}C (68%)[b]	Cal. age ^{14}C (95%)[b]
1330.AL6[c]	230 mg	3042 (± 28)	1381-1343 BC[e] (27%) 1307-1260 BC (38%)	1396-1218 BC (95%)
1330.LS[d]	140 mg	7597 (± 54)	6492-6412 BC (68%)	6589-6378 BC (95%)
1763.AL2[c]	200 mg	3022 (± 23)	1366-1221 BC (68%)	1386-1195 BC (95%)
4564.AL8[d]	145 mg	2072 (± 27)	154-136 BC (11%) 114-46 BC (57%)	175-36 BC (92%)
Sample	Amount of LE	LE Age ^{14}C BP (±1σ)	Cal. age ^{14}C (68%)	Cal. age ^{14}C (95%)
1330.AL6	1.3 mg	2806 (± 28)	996-922 BC (68%)	1044-896 BC (95%)
1330.LS[g]	0.8 mg	122 (± 27)	1685-1707 AD[f] (12%) 1833-1885 AD (31%)	1679-1764 AD (33%) 1801-1897 AD (48%) 1902-1940 AD (15%)
4564.AL8	1.5 mg	1784 (± 25)	215-260 AD (38%) 280-325 AD (30%)	138-264 AD (61%) 274-330 AD (34%)
Sample	Amount of **12**	Miliacin (**12**) Age ^{14}C BP (±1σ)	Cal. age ^{14}C (68%)	Cal. age ^{14}C (95%)
1330.AL2	40 µg	3151 (± 66)	1501-1381 BC (55%)	1560-1259 BC (93%)
1330.AL6	27 µg	2999 (± 87)	1317-1116 BC (57%)	1438-996 BC (95%)
1330.AL10	38 µg	3175 (± 255)	1750-1110 BC (68%)	2044-826 BC (95%)
1763.AL2	15 µg	2967 (± 127)	1307-1015 BC (61%)	1461-894 BC (93%)
4564.AL8	300 µg	1906 (±50)	26-209 AD (68%)	19 BC-236 AD (95%)

[a] BP: "Before Present" where the year 1950, when nuclear weapons testing changed the ^{14}C concentration in the atmosphere, is the reference (0 BP); [b] the radiocarbon content within the atmosphere having varied over time, the calibration atmospheric curve used for the study includes important fluctuations (IntCal13; Reimer et al., 2013). Hence, the ^{14}C age expressed in BP, i.e. before 1950 AD) can be associated with several possible ranges of time for the samples (cal. ^{14}C age BC). The results with the highest statistical probability are reported here and used in Fig. 4, whereas the complete ^{14}C dating data are reported in Table S3 (Supplementary material); [c] measure performed on soil sample after solvent extraction and decarbonation; [d] measure achieved on decarbonated soil sample; [e] BC: Before Christ; [f] A,: Anno Domini; [g] sample likely contaminated by input from recent organic material.

Highlights

•Miliacin (millet biomarker) found in paleosoils filling archaeological structures. •It was ^{14}C-dated after chromatographic isolation. • Hence, millet cropping was dated back to the Bronze Age. •Hollow structures act as "pedological traps" by sealing ancient cultivated soils. •The $\delta^{13}C$ lipid signature was used to decipher the C_3 vs. C_4 plant input to SOM.

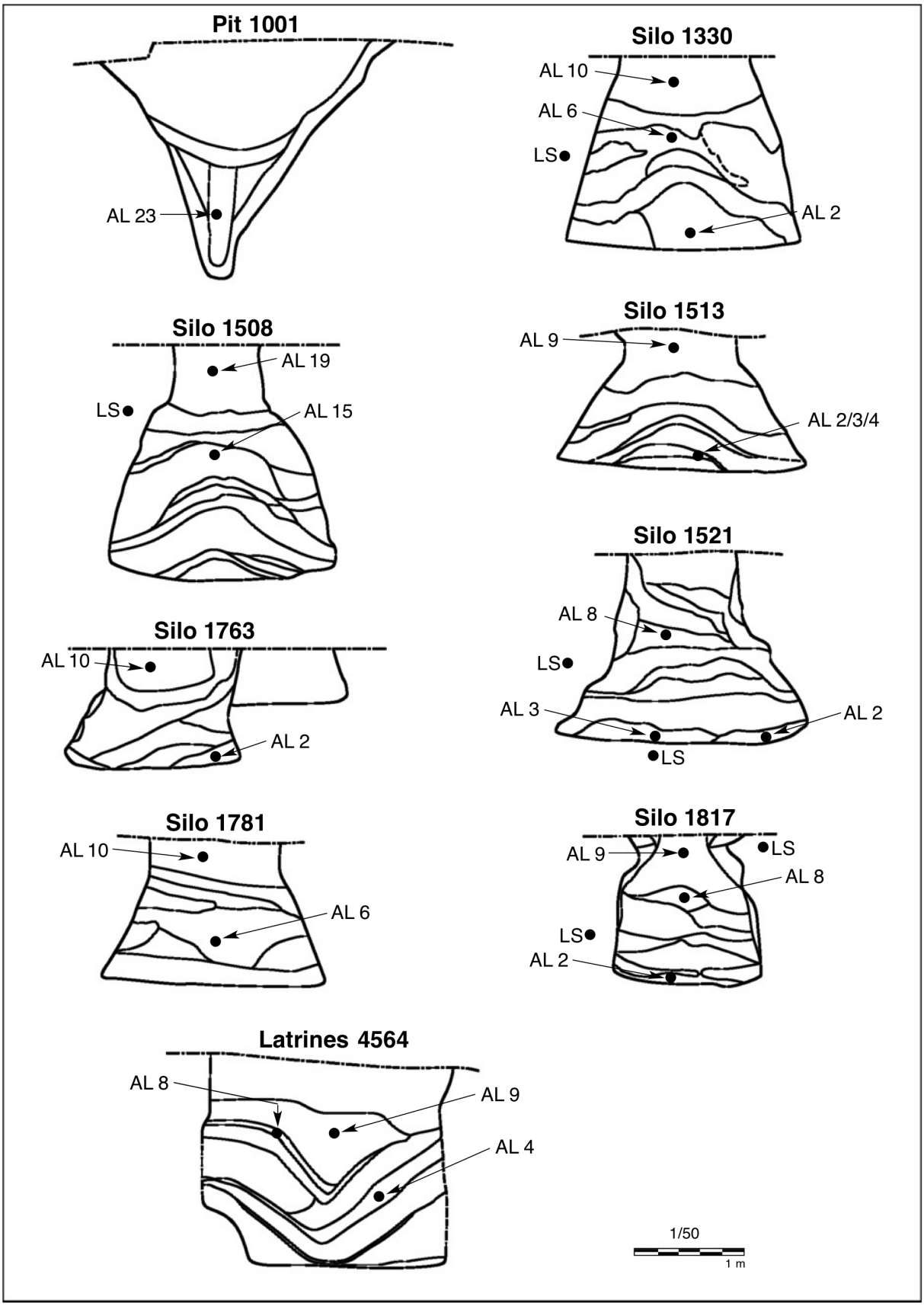

Fig. S1. Archaeological structures and location of samples in the archaeological layers (AL) and loess substrates (LS). Drawing modified after Clément Féliu (INRAP).

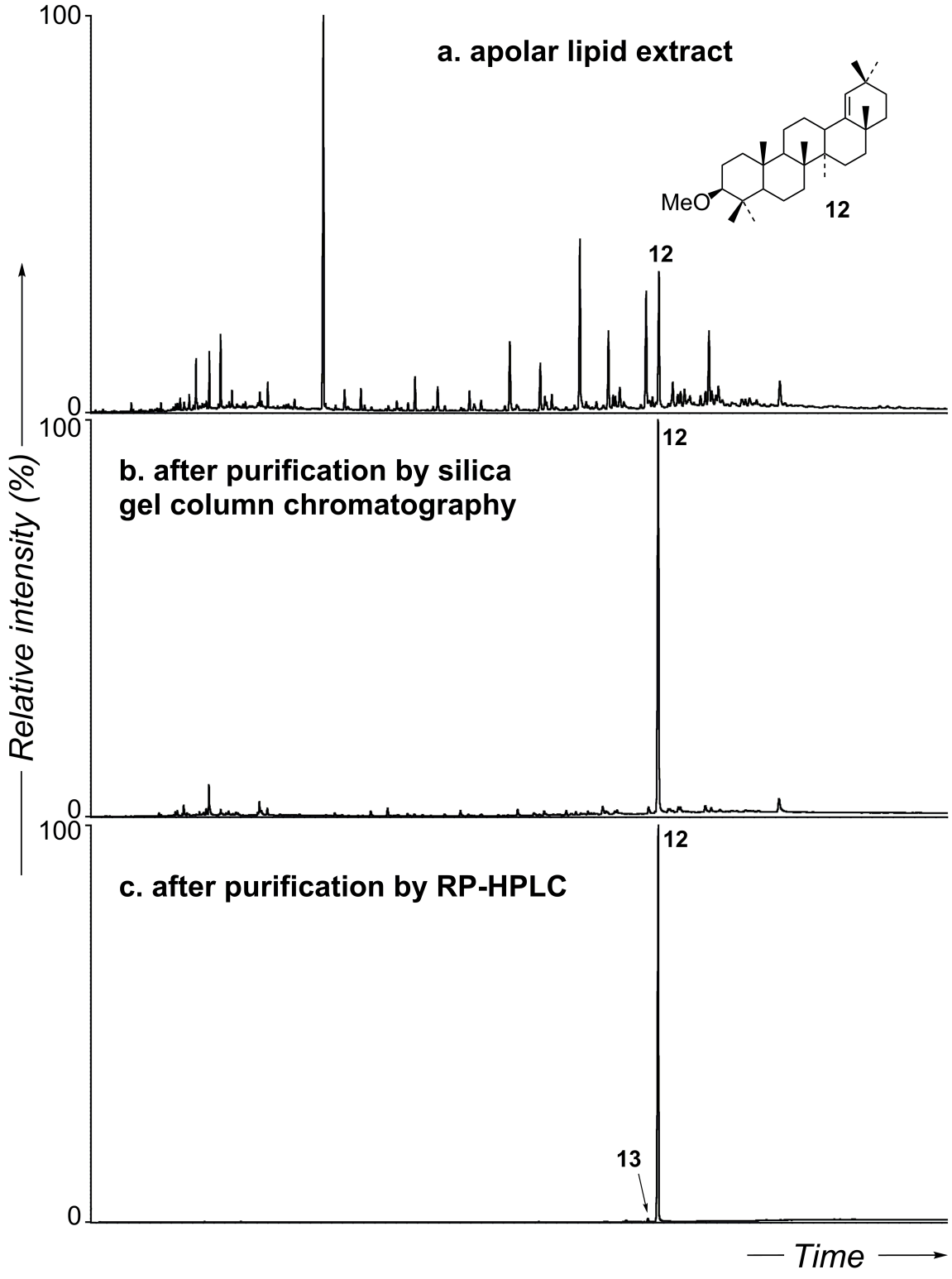

Fig. S2. Gas chromatograms (GC-MS) showing (a) apolar lipid extract from silo 1330.AL2, (b) miliacin-enriched fraction after a separation step using silica gel column chromatography (fraction eluted with CH_2Cl_2; cf. Section 2.6) and (c) isolated miliacin (**12**) after last purification step with RP-HPLC.

Table S1

MS data (EI, 70 eV) of sterols and triterpenoids in lipid extracts from the archaeological soil samples.

Compound	MW[a]	Main MS fragments (*m/z*)	Reference(s)
Stigmasterol (Ac) **1**	454	147 (52), 213 (18), 255 (48), 267 (17), 282 (16), 296 (16), 351 (10), 379 (12), **394 (100)**	Isobe et al. (2002)
Stigmastadienone **2**	410	174 (100), 269 (13), 395 (13), 410 (37)	
β-Sitosterol (Ac) **3**	456	145 (38), 147 (59), 213 (20), 255 (30), 275 (24), 288 (29), 381 (28), **396 (100)**	Isobe et al. (2002)
Glutinone **4**	424	150 (22), 189 (37), 205 (30), 245 (10), **259 (100)**, 274 (57)	Shiojima et al. (1992)
Taraxerol (Ac) **5**	468	189 (42), **204 (100)**, 218 (25), 257 (17), 269 (27), 329 (22), 344 (31), 453 (7), 468 (10)	Shiojima et al. (1992); Lavrieux et al. (2011)
Germanicol (Ac) **6**	468	161 (15), 177 (81), **189 (100)**, 204 (90), 205 (45), 218 (31), 231 (13), 393 (3), 408 (4), 453 (15), 468 (18)	Shiojima et al. (1992); Oyo-Ita et al. (2010)
Lupeol (Ac) **7**	468	175 (38), **189 (100)**, 203 (37), 204 (40), 218 (28), 249 (17), 453 (6), 468 (19)	Shiojima et al. (1992); Stiti et al. (2007)
Friedelin **8**	426	109 (89), **123 (100)**, 125 (52), 163 (56), 191 (48), 205 (45), 246 (44), 273 (39), 302 (17), 341 (8), 411 (17), 426 (23)	Budzikiewicz et al. (1963)
α-Amyrin (Ac) **9**	468	189 (41), 203 (28), **218 (100)**, 249 (5), 408 (3), 468 (4)	Shiojima et al. (1992); Lavrieux et al. (2011)
Bauerenyl acetate **10**	468	**229 (100)**, 241 (20), 289 (94), 301 (12), 393 (7), 408 (7), 453 (8), 468 (5)	Lavrieux et al. (2011)
Betulin (di-Ac) **11**	526	175 (24), 187 (64), **189 (100)**, 191 (59), 203 (41), 216 (28), 249 (6), 393 (7), 423 (19), 451 (9), 466 (33), 526 (1)	Stiti et al. (2007)
Miliacin **12**	440	175 (32), 177 (64), **189 (100)**, 204 (80), 218 (36), 231 (22), 393 (3), 425 (18), 440 (18)	Jacob et al. (2005)
Isosawamilletin **13**	440	175 (7), 189 (14), 203 (50), **218 (100)**, 440 (1)	Jacob et al. (2005)

[a] Alcohols analyzed as acetate derivatives (Ac).

Table S2

^{14}C age (BP[a] and cal. BC/AD[b]) and fraction modern ($F^{14}C$)[c] determined for soil organic matter (SOM), lipid extracts (LE) and isolated miliacin (**12**) from selected silo samples (AL) and loess substrate samples (LS).

Sample	Number (ETH)	Amount of soil	SOM (decarbonated soil) Age ^{14}C BP[a] (± 1σ)	$F^{14}C$[g] (± 1σ)[c]	Cal. age ^{14}C (68.2%)[b]	Cal. age ^{14}C (95.4%)[b]
1330.AL6[d]	ETH-65607	230 mg	3042 (± 28)	0.762 (± 0.003)	1381-1343 BC[f] (27.0%) 1307-1260 BC (37.6%) 1242-1235 BC (3.6%)	1396-1218 BC (95.4%)
1330.LS[e]	ETH-65606	140 mg	7597 (± 54)	0.388 (± 0.003)	6492-6412 BC (68.2%)	6589-6378 BC (95.4%)
1763.AL2[d]	ETH-66449	200 mg	3022 (± 23)	0.687 (± 0.002)	1366-1221 BC (68.2%)	1386-1195 BC (95.4%)
4564.AL8[e]	ETH-65605	145 mg	2072 (± 27)	0.773 (± 0.003)	154-136 BC (11.5%) 114-46 BC (56.7%)	175-36 BC (91.8%) 31-20 BC (1.7%) 12-1 BC (1.9%)
Sample	Number (ETH)	Amount of LE	LE Age ^{14}C BP (± 1σ)	$F^{14}C$ (± 1σ)	Cal. age ^{14}C (68.2%)	Cal. age ^{14}C (95.4%)
1330.AL6	ETH-59648	1.3 mg	2806 (± 28)	0.705 (± 0.002)	996-922 BC (68.2%)	1044-896 BC (95.4%)
1330.LS[h]	ETH-63066	0.8 mg	122 (± 27)	0.985 (± 0.003)	1685-1707 AD[g] (12.3%) 1719-1732 AD (7.0%) 1808-1826 AD (9.4%) 1833-1885 AD (31.5%) 1913-1927 AD (8.0%)	1679-1764 AD (32.7%) 1801-1897 AD (47.8%) 1902-1940 AD (14.9%)
4564.AL8	ETH-63064	1.5 mg	1784 (± 25)	0.801 (± 0.003)	215-260 AD (37.9%) 280-325 AD (30.3%)	138-264 AD (61.0%) 274-330 AD (34.4%)
Sample	Number (ETH)	Amount of **12**	Miliacin (**12**) Age ^{14}C BP (± 1σ)	$F^{14}C$ (± 1σ)	Cal. age ^{14}C (68.2%)	Cal. age ^{14}C (95.4%)
1330.AL2	ETH-59645	40 µg	3151 (± 66)	0.676 (± 0.006)	1501-1381 BC (55.4%) 1342-1306 BC (12.8%)	1607-1582 BC (2.1%) 1560-1259 BC (92.8%) 1242-1234 BC (0.5%)
1330.AL6	ETH-59646	27 µg	2999 (± 87)	0.688 (± 0.008)	1386-1340 BC (11.5%) 1317-1116 BC (56.7%)	1438-996 BC (95.4%)
1330.AL10	ETH-59647	38 µg	3175 (± 255)	0.674 (± 0.021)	1750-1110 BC (68.2%)	2124-2091 BC (0.7%) 2044-826 BC (94.7%)
1763.AL2	ETH-63065	15 µg	2967 (± 127)	0.691 (± 0.011)	1381-1342 BC (6.9%) 1307-1015 BC (61.3%)	1496-1474 BC (1.0%) 1461-894 BC (93.5%) 872-852 BC (0.8%)
4564.AL8	ETH-65602	300 µg	1906 (± 50)	0.789 (± 0.005)	26-209 AD (68.2%)	19 BC-236 AD (95.4%)

[a]BP: "Before Present" where the year 1950, when nuclear weapons testing changed the ^{14}C concentration in the atmosphere, is the reference (0 BP); [b] the radiocarbon content within the atmosphere having varied over time, the calibration atmospheric curve used includes important fluctuations (IntCal13; Reimer et al., 2013). Hence, the ^{14}C age expressed in BP (i.e. before 1950 AD) can be associated with several possible ranges of time for the samples (cal. ^{14}C age BC); [c] $F^{14}C$: fraction modern, $F^{14}C = \exp(-^{14}C age/8033)$; see Reimer et al. (2004); [d] measure performed on soil sample after extraction and decarbonation; [e] measure achieved on decarbonated soil sample; [f] BC: before Christ; [g]AD: Anno Domini; [h] sample likely contaminated by input from recent organic material.

References

Budzikiewicz, H., Wilson, J.M., Djerassi, C., 1963. Mass spectrometry in structural and stereochemical problems. XXXII. Pentacyclic triterpenes. Journal of the American Chemical Society 85, 3688-3699.

Isobe, K.O., Tarao, M., Zakaria, M.P., Chiem, N.H., Minh, L.Y., Takada, H., 2002. Quantitative application of fecal sterols using gas chromatography-mass spectrometry to investigate fecal pollution in tropical waters: Western Malaysia and Mekong Delta, Vietnam. Environmental Science & Technology 36, 4497-4507.

Jacob, J., Disnar, J.-R., Boussafir, M., Albuquerque, A.L.S., Sifeddine, A., Turcq, B., 2005. Pentacyclic triterpene methyl ethers in recent lacustrine sediments (Lagoa do Caçó, Brazil). Organic Geochemistry 36, 449-461.

Lavrieux, M., Jacob, J., Le Milbeau, C., Zocatelli, R., Masuda, K., Bréheret, J.-G., Disnar, J.-R., 2011. Occurrence of triterpenyl acetates in soil and their potential as chemotaxonomical markers of Asteraceae. Organic Geochemistry 42, 1315-1323.

Oyo-Ita, O.E., Ekpo, B.O., Oros, D.R., Simoneit, B.R.T., 2010. Occurrence and sources of triterpenoid methyl ethers and acetates in sediments of the cross-river system, Southeast Nigeria. International Journal of Analytical Chemistry, doi:10.1155/2010/502076.

Reimer, P.J., Brown, T.A., Reimer, R.W., 2004. Discussion: reporting and calibration of post-bomb ^{14}C data. Radiocarbon 46, 1299-1304.

Shiojima, K., Arai, Y., Masuda, K., Takase, Y., Ageta, T., Ageta, H., 1992. Mass spectra of pentacyclic triterpenoids. Chemical and Pharmaceutical Bulletin 40, 1683-1690.

Stiti, N., Triki, S., Hartmann, M.-A., 2007. Formation of triterpenoids throughout *Olea europaea* fruit ontogeny. Lipids 42, 55-67.